BOREAS An international journal of Quaternary research

Glacial and environmental changes over the last 60 000 years in the Polar Ural Mountains, Arctic Russia, inferred from a high-resolution lake record and other observations from adjacent areas

JOHN INGE SVENDSEN, LARS MARTIN B. FÆRSETH, RICHARD GYLLENCREUTZ, HAFLIDI HAFLIDASON, MONA HENRIKSEN, MORTEN N. HOVLAND, ØYSTEIN S. LOHNE, JAN MANGERUD, DMITRY NAZAROV, CARL REGNÉLL AND JOERG M. SCHAEFER

BOREAS

Svendsen, J. I., Færseth, L. M. B., Gyllencreutz, R., Haflidason, H., Henriksen, M., Hovland, M. N., Lohne, Ø. S., Mangerud, J., Nazarov, D., Regnéll, C. & Schaefer, J. M. 2019 (April): Glacial and environmental changes over the last 60 000 years in the Polar Ural Mountains, Arctic Russia, inferred from a high-resolution lake record and other observations from adjacent areas. *Boreas*, Vol. 48, pp. 407–431. https://doi.org/10.1111/bor.12356. ISSN 0300-9483.

Our knowledge about the glaciation history in the Russian Arctic has to a large extent been based on geomorphological mapping supplemented by studies of short stratigraphical sequences found in exposed sections. Here we present new geochronological data from the Polar Ural Mountains along with a high-resolution sediment record from Bolshoye Shchuchye, the largest and deepest lake in the mountain range. Seismic profiles show that the lake contains a 160-m-thick sequence of unconsolidated lacustrine sediments. A well-dated 24-m-long core from the southern end of the lake spans the last 24 cal. ka. From downward extrapolation of sedimentation rates we estimate that sedimentation started about 50–60 ka ago, most likely just after a large glacier had eroded older sediments from the basin. Terrestrial cosmogenic nuclide (TCN) exposure dating (^{10}Be) of boulders and Optically Stimulated Luminescence (OSL) dating of sediments indicate that this part of the Ural Mountains was last covered by a coherent ice-field complex during Marine Isotope Stage (MIS) 4. A regrowth of the glaciers took place during a late stage of MIS 3, but the central valleys remained ice free until the present. The presence of small- and medium-sized glaciers during MIS 2 is reflected by a sequence of glacial varves and a high sedimentation rate in the lake basin and likewise from ^{10}Be dating of glacial boulders. The maximum extent of the mountain glaciers during MIS 2 was attained prior to 24 cal. ka BP. Some small present-day glaciers, which are now disappearing completely due to climate warming, were only slightly larger during the Last Glacial Maximum (LGM) as compared to AD 1953. A marked decrease in sedimentation rate around 18–17 cal. ka BP indicates that the glaciers then became smaller and probably disappeared altogether around 15–14 cal. ka BP.

John Inge Svendsen (john.svendsen@uib.no), Haflidi Haflidason, Morten N. Hovland, Jan Mangerud and Carl Regnéll, Department of Earth Science, University of Bergen, Postbox 7830, Bergen N-5020, Norway and Bjerknes Centre for Climate Research, Jahnebakken 5, Bergen N-5007, Norway; Lars Martin B. Færseth and Mona Henriksen, Faculty of Environmental Sciences and Natural Resource Management, Norwegian University of Life Science, Postbox 503, NO-1432 Ås, Norway; Richard Gyllencreutz, Department of Geological Sciences, Stockholm University, 10691 Stockholm, Sweden; Øystein S. Lohne, Sweco Norway, Fantoftvegen 14P, N-5072 Bergen, Norway; Dmitry Nazarov, Institute of Earth Sciences, St. Petersburg University, St. Petersburg, Russia and A.P. Karpinsky Russian Geological Research Institute (FGBU-"VSEGEI"), 74, Sredny prospect, 199106 St. Petersburg, Russia; Joerg M. Schaefer, Lamont-Doherty Earth Observatory of Columbia University, Palisades, NY 10964, USA; *received 28th March 2018, accepted 17th September 2018.*

The main focus of this paper is the glacial and environmental changes that have taken place in the Polar Ural Mountains of the Russian Arctic during the last Ice Age and towards the present. The landscape development has been reconstructed partly based on the sediment record from Lake Bolshoye Shchuchye (from now on abbreviated Bol. Shchuchye – in English meaning the large pike lake), the largest and deepest lake in the mountain range (Figs 1–3). We have studied the Quaternary deposits in this lake by means of seismic profiling and sediment coring; the seismic profiles revealed 160-m-thick lacustrine sediments in the central and northern parts of the basin. A total of six sediment cores was collected from the lake floor during three subsequent field expeditions (Fig. 3). So far, a 24-m-long sediment sequence (cores 506-48 and -50) from the southern end of the lake has been studied and dated in most detail. An age model based on a series of 27 radiocarbon dates, supported by a sequence of about 5000 annual varves in the lower part, shows that the cored sediments cover a period of about 24 ka without any breaks or disturbances, and provides new insight into the environmental conditions since prior to the Last Glacial Maximum (LGM). The interpretation of the core data is compared with the results of geomorphic and glacial geological investigations in the surrounding area, including 39 *in situ* terrestrial cosmogenic nuclide (TCN) dates (^{10}Be) and 25 Optically Stimulated Luminescence (OSL) dates from exposed sediments (Tables 2, 3 and Figs 2, 3).

We also provide some background information relevant to this study and that serves as a basis for several more specialized papers that utilize this lake record; four are contained in this issue of Boreas (Haflidason *et al.* 2019a,b; Regnéll *et al.* 2019; Lammers *et al.* 2019). Pollen stratigraphical investigations and DNA analyses of molecules derived from plants will be published elsewhere in the near future, whereas results from palaeomagnetic investigation of the lake record are not yet ready for publication.

DOI 10.1111/bor.12356

Fig. 1. A. Digital elevation model of the Polar Urals and the adjacent lowland. Some of the most distinct moraines (white lines), believed to be from the MIS 4 glaciation, are marked (from Svendsen *et al.* 2014). B. Key map showing the location of (A). The ice-sheet extent during the maximum extent of the MIS 2 glaciation is marked (from Svendsen *et al.* 2004). [Colour figure can be viewed at www.boreas.dk]

Background and the state of knowledge

One intriguing outcome of previous research along the northern seaboard of Russia was that there had been larger ice sheets in the Barents-Kara Sea region during MIS 5d–4 than during MIS 2, i.e. opposite to the development of the Scandinavian and most other ice sheets. During an early stage of the last Ice Age (MIS 5d–4) large ice sheets formed over the Barents-Kara Sea region, but their form and dimension varied from time to time, and each of the major glaciations were separated by long-lasting ice-free periods (Mangerud *et al.* 2008b; Möller *et al.* 2015). During the periods around 90 ka (MIS 5b) and 70–60 ka (MIS 4), these ice sheets created major ice-dammed lakes that flooded the lowland on both sides of the Ural Mountains (Mangerud *et al.* 2004; Svendsen *et al.* 2014; Fig. 1). It is controversial as to whether large icecaps formed over the Polar Ural Mountains during the last Ice Age (Astakhov 2013, 2014, 2016, 2018). However, it is clear that outlet glaciers from the mountain range reached the foothills during MIS 4 (Svendsen *et al.* 2014). In contrast to MIS 5d–4, almost the entire Arctic seaboard of Russia to the east of the Arkhangelsk region remained ice free during MIS 2 (Svendsen *et al.* 2004). Widespread steppes that covered much of the Russian Arctic throughout MIS 3–2 then hosted a rich herbivore fauna (Astakhov *et al.* 2004; Hubberten *et al.* 2004; Sher *et al.* 2005) and also a surprisingly early human population (Pavlov *et al.* 2001; Svendsen *et al.* 2010; Slimak *et al.* 2011; Pitulko *et al.* 2017; Hufthammer *et al.* 2019). Perhaps equally surprising, ^{10}Be exposure dating suggests that the tiny cirque glaciers that today exist in the

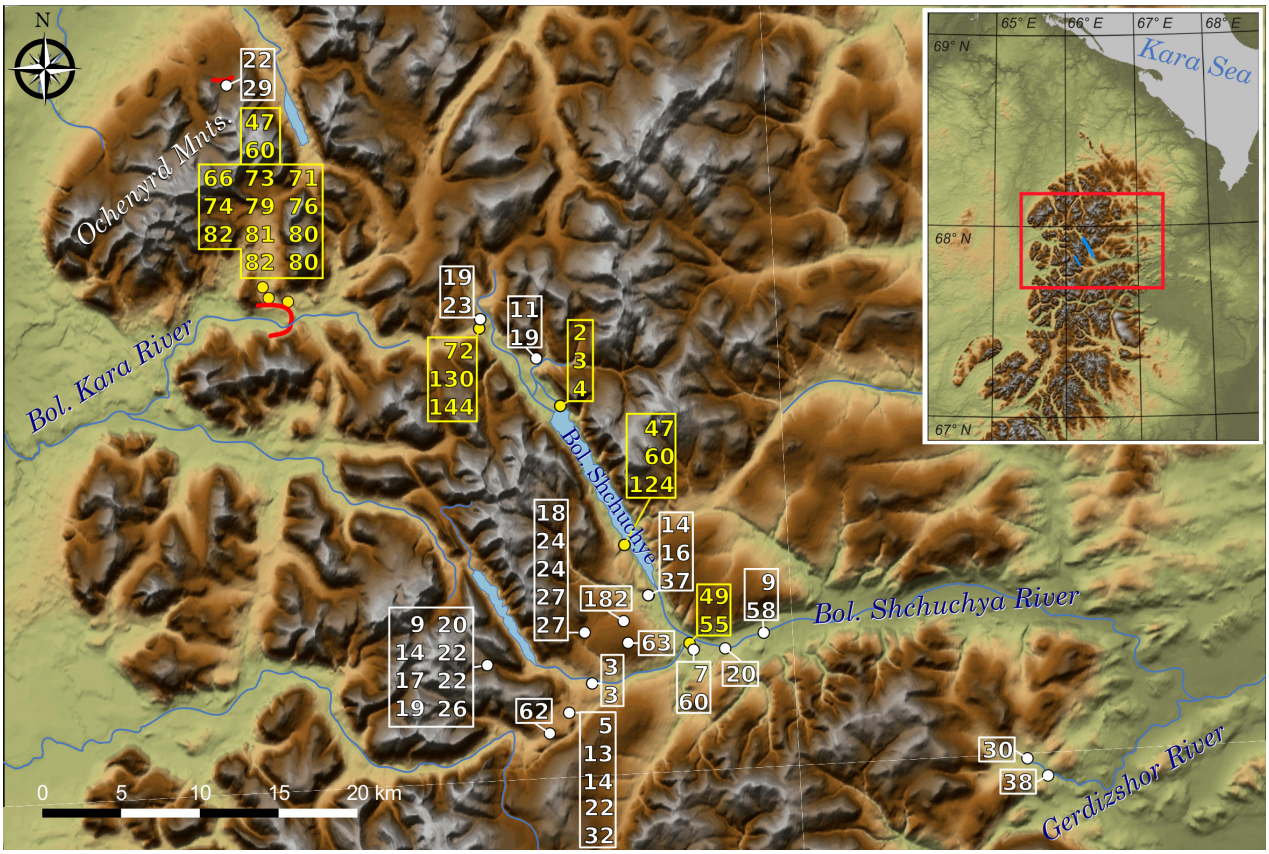

Fig. 2. Map of the study area of the Polar Ural Mountains with OSL (yellow) and ^{10}Be (white) dating sites with rounded ages (ka) marked. The moraine ridges in Bol. Kara river valley and on the northern side of the Ochenyrd Mountains are marked with red lines. A map of the Polar Ural Mountains with study area (red frame) is shown in the upper right corner. [Colour figure can be viewed at www.boreas.dk]

mountains appear to have been only slightly larger during the LGM than today (Mangerud *et al.* 2008a).

Our knowledge of the long-term environmental history of northern Russia is to a large extent based on studies of exposed sections along rivers and the coast (Mangerud *et al.* 1999, 2001; Vasil'chuk *et al.* 2000; Henriksen *et al.* 2001; Astakhov & Svendsen 2002; Svendsen *et al.* 2004; Larsen *et al.* 2006; Astakhov & Nazarov 2010; Schirrmeister *et al.* 2011; Astakhov 2014). Although such sections are useful, the strata are often fragmentary and earlier attempts to reconstruct the palaeo-environment have been hampered by the lack of well-dated continuous records. We have therefore long sought suitable archives from arctic lakes. However, none of the previously cored lakes on the adjacent lowland contained sediments covering the LGM period, even though these landscapes have been permanently ice free since at least 50–60 ka (Svendsen *et al.* 2014). The dating results indicate that lacustrine sedimentation did not start until 15–14 cal. ka BP (Henriksen *et al.* 2003; Paus *et al.* 2003; Väliranta *et al.* 2006) or in some cases not even before the onset of the Holocene (Andreev *et al.* 2005; Sand 2011). Our explanation is that the lake depressions did not form until the permafrost, which in many areas included large bodies of buried glacier ice, started to melt in response to the climate warming. The major melting event appears to have started only after 15 cal. ka BP (the onset of the Bølling interstadial in Western Europe) and was probably further intensified in response to the Holocene warming. The only exception we have experienced was Lake Yamozero on the Timan Ridge farther west, but this lake appears to have dried out for a long period during MIS 2, leading to no sedimentation between 30 and 16 cal. ka BP (Henriksen *et al.* 2008).

The lack of suitable archives in the lowlands turned our focus to lakes in glacially eroded bedrock depressions in the Ural Mountains (Figs 2, 3). If most glaciers here remained small during the LGM, as proposed by Mangerud *et al.* (2008a), some of the lakes should contain long sediment records spanning this period. We therefore cored several mountain lakes during the International Polar Year Program 2007–2008. Cores retrieved from the shallow Lake Gerdizty on the eastern foothills of the mountains reached back to the transition between MIS 4 and MIS 3 at about 65 ka (Svendsen *et al.* 2014). However, the sediment sequence in this basin was thin (3–4 m) and we could not rule out the possibility that there was a break in sedimentation during the LGM, for example if the lake dried out or was frozen to the bottom. In search of more suitable high-resolution archives, we then moved to the much deeper lake basins of Bol. Shchuchye and Malaya

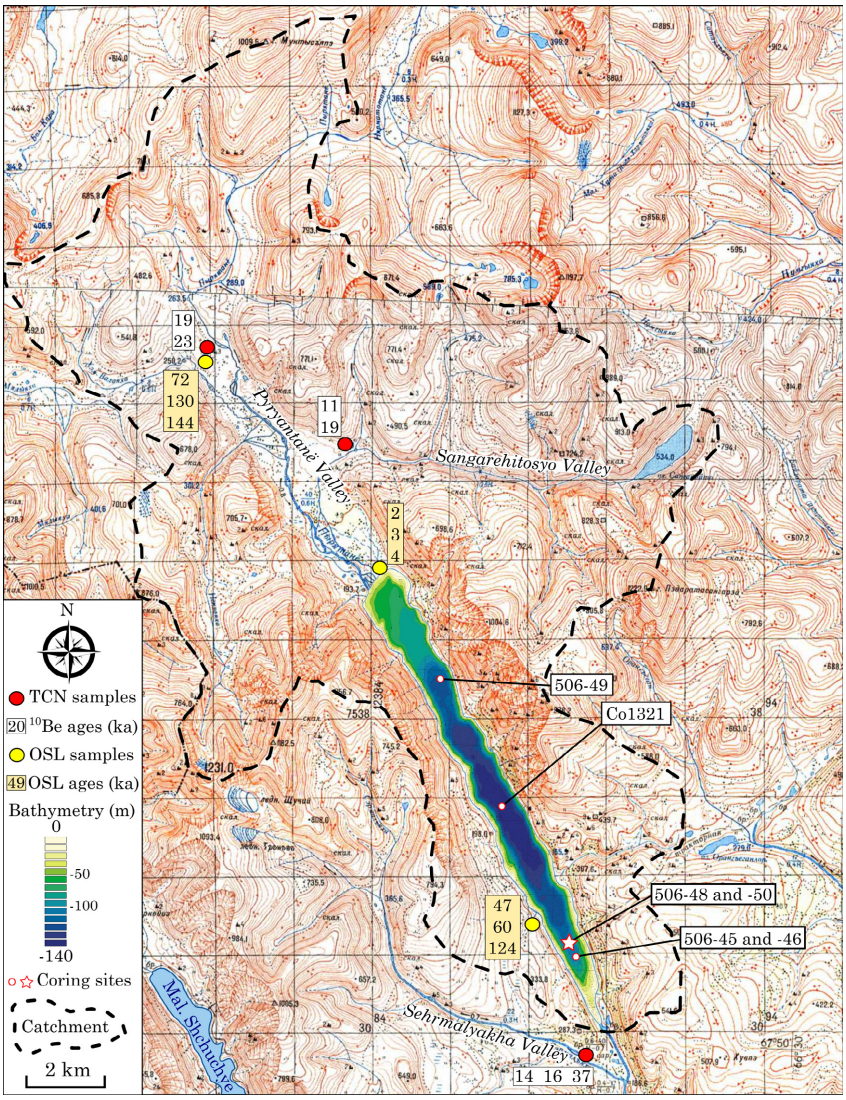

Fig. 3. Bathymetric and topographic map (modified from Map sheet Q-42-1,2 at scale 1:100 000) showing the lake basin of Bol. Shchuchye and its catchment area (contour interval 20 m). The locations of the sediment cores are marked. A 54-m-long core (Co1321) that was retrieved from the central part of the basin by the PLOT project in the year 2016 has not yet been analysed. OSL (yellow) and ^{10}Be ages (ka) (red) that were obtained from adjacent sites are marked. [Colour figure can be viewed at www.boreas.dk]

(Mal.) Shchuchye in the central part of the mountain chain (Figs 1–4). Seismic profiles revealed that the largest and deepest of them, Bol. Shchuchye, contains up to 160-m-thick, acoustically laminated sediments above basement (Haflidason *et al.* 2019a). This discovery opened up entirely new research questions and perspectives that we are now pursuing in collaboration with the German-Russian project Paleolimnological Transect (PLOT).

Study area

Lake Bol. Shchuchye is located in the interior of the Polar Urals (latitude 67°53′24″N, longitude 66°18′36″E), well outside the maximum extent of the Barents-Kara Ice Sheet during MIS 2 (Svendsen *et al.* 2004; Hughes *et al.* 2016). The lake surface is at 187 m a.s.l., and it is located close to the watershed (350 m a.s.l.) between European Russia and Siberia (Figs 2, 3). The highest mountain peaks in this part of the Urals are 900–1200 m a.s.l., many with incised cirques. The lake basin, which is set into a NW–SE trending valley, is bounded by steep rock faces (Fig. 3). Bol. Shchuchye is 13 km long, about 1 km wide and has a maximum water depth of 140 m in the central part. This implies that the bedrock surface underneath the 160-m-thick sediments is located more than 300 m below the present lake level and more than 100 m below sea level. The bedrock on the eastern and northwestern sides of the lake is predominantly Proterozoic-Cambrian basaltic and andesitic rocks whereas the areas to the south and west are underlain by quartzite and phyllitic rocks of Ordovician age (Fig. 5) (Dushin *et al.* 2009). We consider that the lake basin was formed by

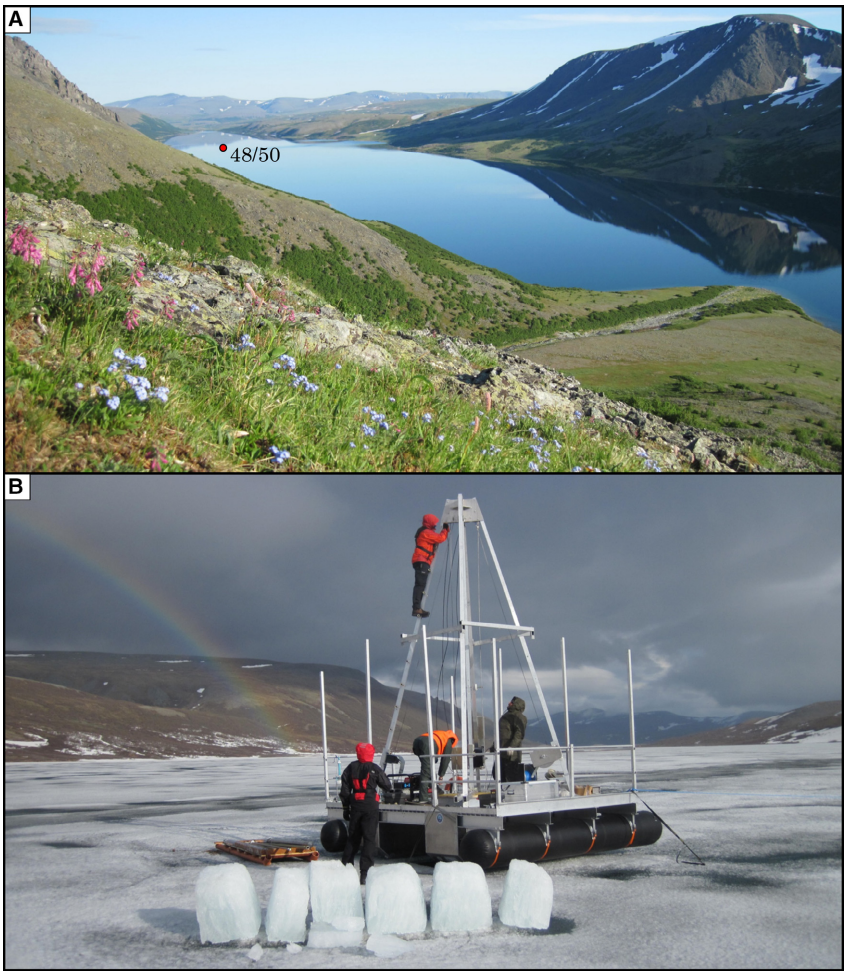

Fig. 4. A. Overview photograph (14 July 2009) of Lake Bol. Shchuchye seen towards the south. The dark green bushes growing on the alluvial fan and on the slope are green alder (*Alnus viridis*). Notice the alluvial fan in the foreground. The location of core sites 48 and 50 in the southern end of the lake is marked with a red dot. B. Photograph of coring raft (28 June 2009) from the ice at site 48 in the southern end of the lake. [Colour figure can be viewed at www.boreas.dk]

glacial erosion during repeated glaciations, following weaknesses along ancient NW–SE striking faults. The bedrock surfaces around the lake show signs of physical weathering, including several metres high tors on the east-facing slopes and in the valley to the north of the lake. Most of the bedrock surfaces above 500–600 m a.s.l. are covered by block fields formed by frost weathering.

Bol. Shchuchye is a cold monomictic lake with thick winter ice and mixing of the water-masses only during the short summer seasons. The catchment, which covers an area of 215 km^2, embraces a narrow zone along the lake as well as a wider hinterland to the north. The main inflow to the lake is the river Pyriatanyu that builds a delta in the northern end. The outlet is in the southern end of the lake and runs via the Bol. Shchuchya River to the much larger Ob River on the West Siberian Lowland.

The climate is cold and continental with thick and continuous permafrost. The mean summer temperature (June-July-August) at the research station Bol. Khadata (260 m a.s.l.), located 25 km to the south of Bol. Shchuchye, is around 7 °C (Solomina *et al.* 2010). The mean annual temperature for the period 1958–1980 was −6° C. The annual precipitation is about 600 mm, slightly more than on the western foothills of the mountain chain. The dominating wind direction is from the west and may cause considerable snow drift during the winter seasons. Around the lake, there are a few tiny cirque glaciers, but they are now almost extinct in response to the recent climate warming. The theoretical snowline in the Polar Urals is estimated to be around 1600 m a.s.l., well above the highest mountain peaks (Troitsky *et al.* 1966). The present glaciers exist because of special local conditions that are favourable for ice-growth, such as mountain shadows that decrease the ablation and wind drift and avalanches that increase the accumulation of snow during the winter season (Mangerud *et al.* 2008a).

The vegetation in the lake surroundings is for the most part thin and patchy and composed of grasses, dwarf shrubs, sedges, mosses and lichens (Fig. 4A). On the south-facing slopes there are thickets of green alder

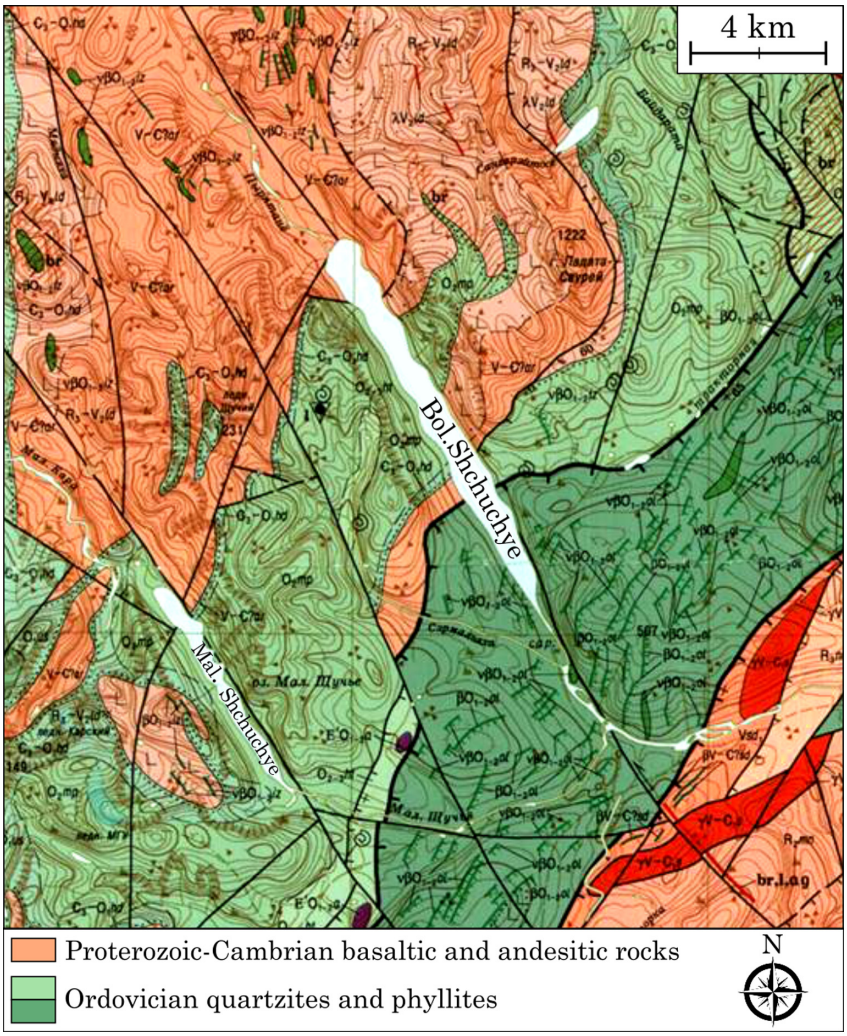

Fig. 5. Map of the bedrock geology in the area around Bol. Shchuchye and Mal. Shchuchye. Fault lines are marked with black lines. Simplified from Dushin *et al.* (2009). [Colour figure can be viewed at www.boreas.dk]

(*Alnus viridis*), a small bush-shaped tree that on the south-facing slopes may grow up to an elevation of around 300 m a.s.l. There are no other trees growing in the catchment, but local stands of larch (*Larix sibirica*) were observed a few km to the southeast of the lake.

Material and methods

We have studied the glacial history of the Polar Urals by using satellite images, aerial imagery, and direct observations in the field. We carried out geological fieldwork in 2007 and 2009, describing exposed sections and landforms, and collecting samples for OSL dating and ^{10}Be surface exposure dating. Exact location and elevation were determined with a hand-held GPS.

Seismic surveying and coring of the lake floor sediments

We mapped the sediment distribution with seismic methods, including a Sparker and sub-bottom profiler during the summer of 2007; methods and results are described by Haflidason *et al.* 2019a). In 2007, we also collected three short cores that were up to 3.2 m long (506-45, -46, -47) by using a light piston-coring device (Table 1, Fig. 4B). However, as seismic profiles revealed that the basin contains up to 160 m of acoustically laminated sediments (Fig. 6), another coring expedition was organized in 2009 with sampling equipment capable of retrieving much longer cores. We then used a UWITECH Piston Corer with 2-m-long and 10-cm-diameter PVC sample tubes for most of the sections (http://www.uwitec.at), but 9-cm steel tubes for some parts. A cone resting on the lake floor allowed re-entry, reducing the friction and thus allowing deeper coring by taking 2-m-long core segments continuously down into the same hole. As the sampler was being fed into the hole, the piston remained fixed to the sampler. The moment the sampler reached the desired depth where we wanted to cut the next core segment, the piston was disconnected after which the sampler was hammered further down with weights hitting the connecting rods from above.

The uppermost 20–30 cm of the 2-m-long core sections was in many cases deformed, and this disturbed segment probably was sucked into the sampler the moment the cutting started. We think this is due to a higher pressure in the sediment column at these depths than in the water-filled tube inside the sampler so that some sediment became squeezed into the sample tube the moment the piston was disconnected from the sampler. To ensure full recovery a parallel core (506-50) was therefore taken close by core 506-48 in such a way that each parallel core section from the two holes overlaps by about 30–40 cm (Fig. 7).

The core locations were selected from the seismic profiles. Because 0.5 m of winter ice still covered the lake when we arrived in the area in late June (Fig. 4B), we cored the first site (core 506-48) in the southern end of the lake (67°51′22.248″N, 66°21′30.096″E) from a raft that was pushed on the ice to the predetermined position (Figs 3, 4A). Two additional sites were cored from the raft after the ice melted away in early July; core 49 (67°54′47.232″N, 66°16′32.988″E) in the northern part of the lake and core 50 taken only about 20 m away from core 48. Cores 48 and 50 can be correlated in detail based on the lamination structures and they jointly represent a continuous succession throughout the cored sequence, except for a core gap of 40 cm between the two deepest segments of core 48 (Fig. 7).

The core segments from each site are numbered from the top and labelled with increasing numbers downwards (506-48-01, 506-48-02, etc.), although the project number (506) is often omitted in the text. Each 2-m-long core segment was cut into two halves, labelled 01 (upper half) and 02 (lower half) (e.g. 48-01-01 and 48-01-02). All depths are measured from the top of the cored sequence at each site, accepting that this zero point is located somewhat below the present lake floor, for example 50–70 cm for core 48. The uppermost sequence was not sampled with the piston-corer because the bottom frame of the entrance cone pushed some of the soft surface sediments away as it was lowered to the lake floor. Instead, we used a specially designed UWITEC gravity corer to collect a 60-cm-long, 60-mm-diameter, undisturbed sample of the surface sediments. Unfortunately, this short surface core from site 48 was lost during transportation, and a new short core was therefore collected from the winter ice in 2016. The latter core, which is 42 cm long, has been used to extend the results from core 48 and further up to the surface at the lake floor. We stored, handled and transported the cores well above 0 °C to avoid freezing.

Documentation of the sediment cores

After arrival in Bergen, the cores were split length-wise, photographed and described. Magnetic susceptibility (MS) was measured using a GEOTEK Multisensory Core Logger, and major elements were analysed using an ITRAX X-Ray Fluorescence (XRF) Core Scanner (Croudace *et al.* 2006), at a spatial resolution of 0.5 mm. Grain size, loss on ignition, varve counting and a more detailed description of the sedimentology and geochemistry is provided by Regnéll *et al.* (2019).

Radiocarbon dating

The chronology is to a large extent based on accelerator mass spectrometry (AMS) ^{14}C measurements of 27 samples from core 506-48, all conducted on hand-picked pieces of plant remains (Table 1). In addition, five dates are available from a short (3.2 m) core (506-46) that was taken 600 m further to the south (Figs 3, 7). With a few exceptions within the Holocene sequence, we could not observe plant macrofossils by the naked eye on the sediment surface. We therefore cut out about 2-cm-thick sediment slices that comprise about ¼ of the half-core cross-section area, i.e. about 20 cm^3. However, sometimes we had to double the volume to obtain enough material for dating. The samples were washed on 125-µm sieves using distilled water and transferred to a glass dish with distilled water. Many samples were treated this far, and those with the most plant remains were selected for the next step. Plant fragments were picked with tweezers and Pasteur pipette under a stereo-microscope, dried at 105 °C and then stored in a freezer. The samples were always covered to avoid dust and other contamination. Most plant remains had a maximum diameter of only about 1 mm, and we submitted all the plant fragments that were picked from each sample, typically 30–40 pieces. We assume that all samples consist of terrestrial plant remains, but all pieces were too small for taxon identification. The exception is the sample Poz-69671, where one single, 0.5-cm-long, twig of willow was found. All samples were dated at the Poznan (Poz) radiocarbon laboratory in Poland, except a few measured by Beta Analytic (Table 1). All ages were calibrated using the INTCAL13 calibration curve (Reimer *et al.* 2013) and the online Calib program (Stuiver *et al.* 2017).

Optically Stimulated Luminescence (OSL) dating

A series of 25 OSL samples was collected from sedimentary sections in the area around the lake (Table 2) using opaque PVC tubes hammered into freshly exposed sediment layers Fig. 2). The samples were analysed at the Nordic Laboratory for Luminescence Dating (Aarhus University) at Risø National Laboratory, Denmark. The measurements of quartz grains were done in large aliquots in the sand size fraction (180–250 µm) using a standard Risø OSL reader equipped with blue light (470 nm, ~50 nW cm^{-2}) stimulation. The equivalent dose measurements follow the single aliquot regenerated (SAR) dose protocol (Murray & Wintle 2000; Mangerud *et al.* 2001) with a 260 °C (10 s) and 220 °C thermal pretreatment before the natural/regenerated signals and

Table 1. ^{14}C ages from Bol. Shchuchye. The dating was conducted by the Poznan (Poz) radiocarbon laboratory in Poland and Beta Analytic (Beta).

Sample depth (cm)	Mean depth (cm)	Sample weight (mg)	Weight C (mg)	Radiocarbon Lab.-ID	Conventional ^{14}C ages (a BP)	1σ	Calibrated ages (cal. a BP)				
							65% conf. interval		95% conf. interval		Median
							From	To	From	To	
Core 506-48											
4–5	4.5	25.7		Poz-79407	1480	30	1336	1339	1306	1411	1364
64–66	65	6.1		Poz-69670	2285	30	2211	2348	2163	2352	2321
112.5 –114.5	113.5	1.3	0.3	Poz-79408	2645	35	2746	2777	2736	2844	2764
172–173	172.5	1.9	0.5	Poz-79409	3730	35	3993	4147	3975	4224	4080
209–210.5	210	105.6		Poz-69671	4565	35	5074	5318	5053	5441	5194
262–263	262.5	16.5	0.6	Poz-79410	5890	40	6665	6745	6575	6830	6711
350.5–351.5	351	77.3	0.5	Poz-69673	7750	60	8457	8588	8415	8630	8524
434.5–435.5	435	1.2	0.2	Poz-79412	9700	70	10 878	11 217	10 785	11 240	11 107
469–470	469.5	5.6		Poz-79413	10 010	50	11 353	11 612	11 273	11 717	11 495
553	553			Beta-282484	10 560	50	12 429	12 616	12 410	12 661	12 542
622–623	622.5			Beta-473334	12 040	40	13 794	13 946	13 760	14 028	13 885
622–623	622.5			Beta-473333	12 310	40	14 071	14 566	14 117	14 333	14 245
718–720	719	6.1		Beta-282485	12 700	50	15 054	15 228	14 894	15 303	15 132
785–786	785.5			Beta-473335	13 020	50	15 466	15 718	15 331	15 793	15 590
867–869	868	4.9	0.13	Poz-79403	14 300	140	17 205	17 602	17 014	17 820	17 410
960–962	961		0.3	Poz-69674	14 390	100	17 390	17 685	17 225	17 847	17 538
1097.5–1101.5	1099.5	11.7	0.2	Poz-69675	15 030	130	18 092	18 428	17 947	18 576	18 264
1170.5–1178.5	1174		0.6	Poz-69677	15 660	90	18 801	18 990	18 722	19 136	18 904
1285–1287	1286			Beta-282486	15 180	60	18 365	18 535	18 278	18 620	18 450
1531–1536	1533.5	3.9	0.3	Poz-69678	17 620	150	21 068	21 524	20 880	21 756	21 305
1722–1724	1723	4.5	0.2	Poz-79414	17 400	150	20 784	21 229	20 597	21 450	21 010
1879–1884	1881.5	2.7	0.2	Poz-79415	20 600	210	24 508	25 105	24 248	25 368	24 809
1879–1884	1881.5		0.4	Poz-69679	25 520	270	29 282	30 065	28 967	30 438	29 668
1933–1937	1935	2.2	0.13	Poz-79404	18 370	210	21 979	22 432	21 711	22 668	22 210
2052–2056	2054	2.5	0.11	Poz-79405	16 700	170	19 946	20 384	19 697	20 566	20 153
2339–2342	2340.5	19.8	0.7	Poz-69680	20 380	120	24 268	24 676	24 144	24 956	24 494
2339–2342	2340.5	3.9	0.15	Poz-79406	18 750	170	22 440	22 803	22 299	23 036	22 632
Core 506-46											
116	116	9.2		Poz-23694	5550	35	6300	6394	6292	6402	6346
180–181	180.5	2.4		Poz-23695	7610	50	8375	8444	8345	8537	8410
219–220	219.5	5.3		Poz-23696	8570	50	9499	9554	9474	9656	9537
249–250	249.5	8.8		Poz-23697	9380	50	10 555	10 683	10 442	10 734	10 610
294–295	294.5	8.6		Poz-23698	10 710	60	12 625	12 712	12 567	12 727	12 663

the test dose signals, respectively. The samples were held at 125 °C during stimulation. The water content and dose rates were measured in the Risø laboratory by using high-resolution gamma spectrometry and beta counting. For the calculations of total dose rates, it was assumed that the sediments were saturated by water or ice throughout the burial period. The samples fulfil standard quality checks of the reported dates, such as dose recovery, which were routinely done in the Risø dating laboratory.

Terrestrial cosmogenic nuclide (TCN) exposure dating

We present 39 previously unpublished ^{10}Be ages (Table 3). All but four samples were collected with chisel and hammer, the rest by drilling, and were taken from the top surfaces of exposed boulders of quartzite and gneiss (Gosse & Phillips 2001). Topographic shielding was measured in the field by using a compass with clinometer. We selected boulders with low-relief tops that showed only weak or moderate signs of weathering. Most dated boulders were at least 0.4 m high and more than 0.5 m across. With the exception of two samples (98-0034 and 98-0035), all were processed for ^{10}Be measurement at the Lamont-Doherty Earth Observatory (LDEO) Cosmogenic Nuclide Laboratory, following the procedure prescribed by Schaefer *et al.* (2009). Samples 98-0034 and -0035 were processed for ^{10}Be at Dalhousie University, Canada, following the procedure given in Mangerud *et al.* (2008a). The ^{10}Be ages were calculated using the CRONUS-Earth online exposure age calculator (Balco *et al.* 2008). We adopted a regionally constrained production rate (3.91±0.19 atoms g^{-1} a^{-1}) for northeastern North America (Balco *et al.* 2009), but notice that none of the conclusions depends on the choice of the ^{10}Be production rate. It can be mentioned in this context that this production rate is almost identical to the Arctic-wide rate determined by Young *et al.* (2013).

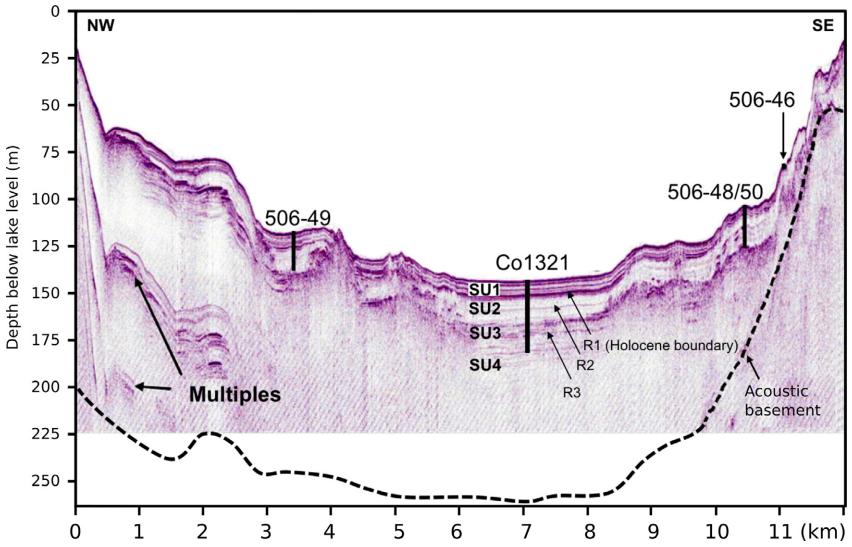

Fig. 6. Interpreted seismic (sparker) longitude profile from Bol. Shchuchye. The core sites are marked. The acoustic basement, interpreted as the bedrock surface (based on seismic cross-profiles), is marked with a stippled line. [Colour figure can be viewed at www.boreas.dk]

Results

Lithostratigraphy of the lake cores

The overlapping cores 506-48 and -50 were retrieved only about 20 m apart at a water depth of 105 m. They can be correlated in detail based on colour images, lamination pattern, palaeomagnetism, and XRF element analyses (Regnéll *et al.* 2019), and form an uninterrupted composite record. Core 48 reached a sediment depth of 24 m whereas core 50 stopped at a depth of 20.95 m (Figs 7, 8).

Core 48 reaches down to a distinct reflector that marks the upper boundary of a seismic unit with a chaotic internal structure and which in places has a somewhat bumpy surface (Fig. 6). During coring, the sampler penetrated into the sediments corresponding to this unit, but due to technical problems the core catcher was not released and the sediments slid out of the tube when the sampler was pulled up. A number of distinct scratch marks were inflicted on the PVC piston during this sampling attempt and the only explanation is that the sediments just below the core depth of 24 m contain many sharp-edged pebbles, in stark contrast to the overlying strata that only contain sand and finer particles. The genetic interpretation of the mentioned seismic unit is uncertain, but we suspect that it is either a coarse-grained glacial deposit or a slide deposit.

The cored sequence (48/50) is divided into three lithostratigraphical units labelled A to C from the surface, and is here briefly described in chronological order from the oldest to the youngest (Fig. 8). The sediments in all three units are characterized by a near homogenous grain-size distribution, ranging from a median diameter (D50) of 5 to 15 μm, i.e. fine silt.

Unit C, from 24.00 to 11.40 m, consists of finely laminated sediments, or rhythmites, each couplet commonly 1–5 mm thick (Fig. 9). Each couplet is composed of a greyish silty lamina at the base followed by a thinner brownish lamina at the top. As discussed in Regnéll *et al.* (2019) these couplets are interpreted as annual varves. The rhythmites are occasionally interrupted by thicker layers (5–20 mm) of fining up sequences from sand to silt, interpreted as turbidites. There are no signs of deformation or erosion below the turbidite layers.

Unit B, from 11.40 to 6.55 m is a transitional unit, characterized by alternating sections with distinct rhythmic laminations, similar to those in unit C, and more diffusely laminated sections. The laminations (rhythmites) become less distinct and more incoherent upwards in the succession, with a gradual transition to unit A above.

Unit A, from 6.55 to 0 m, is diffusely layered and partly massive with a light grey colour (Fig. 10). The content of organic matter is still low, but macroscopic plant remains occur more frequently as compared with the sediments below. Unit A contains turbidite layers similar to the ones in units B and C, but somewhat thicker (10–30 mm) with the thickest ones up to 70 mm thick.

Chronostratigraphy of the cored sequence

An age model for the cores 48/50 has been constructed based on the 27 AMS radiocarbon ages (Table 1) and using the program CLAM version 2.2 (Fig. 8; Blaauw 2010). We applied a 0.4 smooth spline function to fit the series of calibrated radiocarbon ages. However, for the sequence below 11.40 m we consider that a floating varve chronology provides a more precise internal chronology. For the final age-depth curve we have therefore combined the age model based on radiocarbon ages with the varve

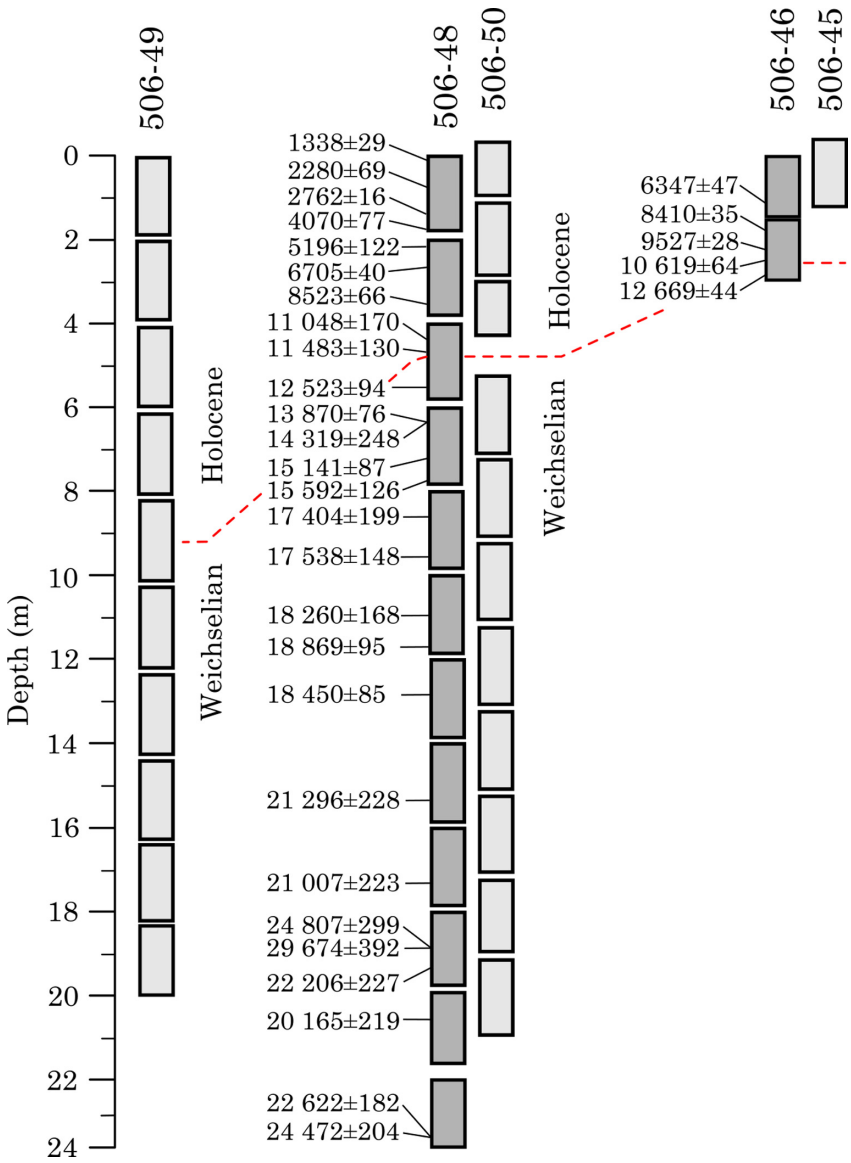

Fig. 7. Depth intervals of the overlapping segments of the two neighbour cores 48 and 50 and those from cores 46 and 49. The calibrated radiocarbon dates (cal. a BP) are marked on the core sections. [Colour figure can be viewed at www.boreas.dk]

chronology of unit C, as explained by Regnéll *et al.* (2019). The Vedde Ash, a widespread tephra horizon that originates from a volcanic eruption in Iceland in the middle of the Younger Dryas (Mangerud *et al.* 1984), has been identified at a sediment depth of 5.11–5.12 m in core 48, and this stratigraphical position fits very well with the age model (Haflidason *et al.* 2019b).

The varve-part of the age model starts at the top of unit C (Regnéll *et al.* 2019), and this anchoring point for the floating varve chronology has been assigned an age of 18 679±128 cal. a BP as defined by the series of radiocarbon dates from the sequence above. Below this level (11.40 m) there are 5134±178 annual varves and, accordingly, we conclude that the bottom end of the core has an age of 23 813±306 cal. a BP (Regnéll *et al.* 2019). Also, this basal age fits well with the radiocarbon dates (Fig. 8).

Shorelines along the margins of Bol. Shchuchye

A narrow terrace that is located about 8 m above the present lake level is partly cut into bedrock and can be traced discontinuously along the western shore of Bol. Shchuchye. This ledge is 20–30 m at the widest and is locally bound by a 2–3 m high cliff along its back edge. In some places, it is covered by a thin veneer of gravel consisting partly of disc-shaped and somewhat rounded stones. The ledge is partly covered by slope deposits and is not clear everywhere. We interpret this terrace as a former shoreline,

Table 2. Optically Stimulated Luminescence (OSL) dates on quartz grains using the sand size fraction obtained at the Nordic Laboratory for Luminescence Dating, Risø, Denmark.

Risø lab. no.	Field no. ICEHUS-	Depth (cm)	Material and setting	Age±1σ (ka)	Equivalent dose (Gy)	n	Annual dose rate (Gy ka^{-1})	w.c. (%)
112503	09-5021	75	Gravelly beach deposits in low terrace at NW shore of Bol. Shchuchye	3.0±0.4	3.9±0.4	31	1.27±0.06	12
112504	09-5022	130	Gravelly beach deposits in low terrace at NW shore of Bol. Shchuchye	3.8±0.4	6.9±0.6	34	1.83±0.07	26
112505	09-5041	275	Gravelly beach deposits in low terrace at NW shore of Bol. Shchuchye	2.4±0.3	4.1±0.5	28	1.74±0.08	22
112501	09-5019	30	Fluvial sand in meltwater channel W of Bol. Shchuchye	29±2	64±3	27	2.23±0.09	24
112502	09-5020	25	Fluvial sand in meltwater channel W of Bol. Shchuchye	57±4	129±8	37	2.25±0.09	20
112506	09-6014	45	Fluvial sand in meltwater channel W of Bol. Shchuchye	55±6	119±11	17	2.18±0.09	21
112513	09-7008	90	Sandur deposit in Pyryantanë River valley, NW of Bol. Shchuchye	144±12	215±16	24	1.49±0.06	21
112514	09-7009	90	Sandur deposit in Pyryantanë River valley, NW of Bol. Shchuchye	72±9	112±14	22	1.56±0.06	22
112515	09-7010	90	Sandur deposit in Pyryantanë River valley, NW of Bol. Shchuchye	130±11	212±15	24	1.63±0.07	23
082512	07-7009	1600	Sand in lower part of fluvial terrace, Bol. Kara Valley	74±5	95±4	18	1.28±0.06	28
082513	07-7010	1550	Sand in lower part of fluvial terrace, Bol. Kara Valley	66±4	99±4	18	1.49±0.07	26
082514	07-7011	1500	Sand in lower part of fluvial terrace, Bol. Kara Valley	82±5	102±5	30	1.24±0.05	36
082515	07-7012	850	Glaciolacustrine sand and silt, distal part of moraine in Bol. Kara Valley	80±5	106±5	18	1.32±0.05	31
082516	07-7013	800	Glaciolacustrine sand and silt, distal part of moraine in Bol. Kara Valley	71±4	100±4	18	1.42±0.06	29
082517	07-7014	600	Glaciolacustrine sand and silt, distal part of moraine in Bol. Kara Valley	80±4	123±3	21	1.54±0.06	31
082518	07-7015	550	Glaciolacustrine sand and silt, distal part of moraine in Bol. Kara Valley	76±4	112±4	17	1.48±0.06	33
082519	07-7016	250	Glaciolacustrine sand and silt, distal to moraine in Bol. Kara Valley	47±3	81±3	18	1.73±0.07	25
082520	07-7017	250	Glaciolacustrine sand and silt, distal to moraine in Bol. Kara Valley	60±3	104±3	18	1.74±0.07	30
082521	07-7018	800	Glaciolacustrine sand and silt, distal to moraine in Bol. Kara Valley	79±5	125±6	18	1.57±0.06	32
082522	07-7019	900	Glaciolacustrine sand and silt, distal to moraine in Bol. Kara Valley	82±5	129±4	32	1.56±0.06	33
082523	07-7020	1100	Glaciolacustrine sand and silt, distal to moraine in Bol. Kara Valley	73±4	122±2	20	1.67±0.07	30
082524	07-7021	1200	Glaciolacustrine sand and silt, distal to moraine in Bol. Kara Valley	81±5	111±5	30	1.37±0.06	32
112507	09-6015	580	Delta forest along Bol. Shchuchya River	75±3	75±3	23	1.30±0.06	13
112508	09-6016	570	Delta forest along Bol. Shchuchya River	62±5	103±7	34	1.67±0.07	29
112509	09-6017	240	Delta topset along Bol. Shchuchya River	49±4	91±7	26	1.85±0.08	20

an interpretation that is supported by a 'staircase' of indisputable beach ridges from the present shore and up to this level in the southern end of the lake. The age is uncertain as we have no dating results from this shore level. However, as will be explained below, it appears that a relict glacifluvial fan near the southern end of the lake was deposited to this level (Fig. 10A). Exposure dates conducted on boulders from the surface of this fan suggest that the

Table 3. ^{10}Be dates from the study area in the Polar Urals. The samples were geochemically processed and beryllium separated at the ^{10}Be measurement at the Lamont-Doherty Earth Observatory (LDEO), Cosmogenic Nuclide Laboratory at Columbia University. The Be isotope measurements were performed by the Center for Accelerator Mass Spectrometry at the Lawrence Livermore National Laboratory (CAMS), relative to the widely used 07KNSTD standard. Given uncertainties reflect 1σ analytical errors. Other sources of error include the value of the ^{10}Be production rate of ~4% and the value of the Lamont ^{9}Be spike (about 1%).

Sample ICEHUS-	Boulder type	Boulder height (cm)	Lat. (°N)	Long. (°E)	Elevation (m a.s.l.)	Sample thickness (cm)	Location, geomorphological setting	^{10}Be (at g^{-1})	1σ	AMS Std	^{10}Be age (ka)
09-5031	Quartzite	13	67.83197	66.37200	220	2.5	Sehrmalyakha sandur	1.8469E+05	3.6938E+03	07KNSTD	37.04±0.75
09-5032	Quartzite	20	67.83195	66.37257	210	5	Sehrmalyakha sandur	7.8375E+04	2.0377E+03	07KNSTD	15.80±0.41
09-6013	Quartzite	15	67.83197	66.37200	217	5	Sehrmalyakha sandur	7.2260E+04	3.3962E+03	07KNSTD	14.45±0.68
09-5037	Quartzite	23	67.98975	66.12121	269	4.5	Pyriatanyu sandurs	1.2341E+05	3.7022E+03	07KNSTD	23.43±0.71
09-5038	Quartzite	35	67.98981	66.12124	270	2.5	Pyriatanyu sandurs	1.0172E+05	3.0517E+03	07KNSTD	19.28±0.58
09-5034	Quartzite	30	67.96728	66.20575	269	5	Sangareytosyu alluvial fan	9.9867E+04	2.6964E+03	07KNSTD	18.94±0.51
09-5035	Quartzite	17	67.96728	66.20575	269	2.5	Sangareytosyu alluvial fan	5.9814E+04	1.7944E+03	07KNSTD	11.32±0.34
09-5049	Quartzite	40	67.76336	66.25590	340	3.5	Main watershed, moraine	1.7970E+05	3.4143E+03	07KNSTD	31.85±0.61
09-5050	Quartzite	35	67.76383	66.25614	346	4.5	Main watershed, moraine	7.7351E+04	2.0885E+03	07KNSTD	13.57±0.37
09-5051	Quartzite	35	67.76499	66.25550	344	3.5	Main watershed, moraine	7.5097E+04	2.0276E+03	07KNSTD	13.20±0.36
07-5016	Quartzite	45	67.76743	66.23415	428	5	Main watershed, moraine/kame ridge	1.3571E+05	4.8612E+03	07KNSTD	21.77±0.78
07-5018	Quartzite	80	67.77237	66.23990	435	5	Main watershed, terrace-like surface	3.1728E+04	2.3991E+03	07KNSTD	5.04±0.38
07-7032	Quartzite	170	67.75375	66.22214	425	5	Main watershed, hill (riegel)	3.8029E+05	7.2242E+03	07KNSTD	61.64±1.19
09-5042	Quartzite	140	67.79360	66.11918	667	5	MGU glacier, outer moraine	1.4518E+05	2.7584E+03	07KNSTD	18.73±0.36
09-5043	Quartzite	125	67.79344	66.11879	665	3.5	MGU glacier, outer moraine	7.0251E+04	1.3348E+03	07KNSTD	9.06±0.17
09-5044	Quartzite	100	67.79394	66.11607	683	5	MGU glacier, outer moraine	2.0384E+05	3.8730E+03	07KNSTD	25.95±0.50
09-5057	Quartzite	-	67.79253	66.11227	669	-	MGU glacier, inner moraine	1.7025E+05	3.1810E+03	07KNSTD	21.9±0.4
09-5060	Quartzite	60	67.79038	66.12361	624	4.5	MGU glacier, inner moraine	1.0587E+05	2.0116E+03	07KNSTD	14.20±0.27
09-5061	Quartzite	-	67.78952	66.11441	606	-	MGU glacier, inner moraine	1.5883E+05	3.2394E+03	07KNSTD	21.7±0.5
09-5062	Quartzite	-	67.78951	66.1148	617	-	MGU glacier, inner moraine	1.2423E+05	2.1027E+03	07KNSTD	16.8±0.3
09-5063	Quartzite	-	67.78862	66.12251	595	-	MGU glacier, inner moraine	1.4134E+05	2.7656E+03	07KNSTD	19.5±0.4
09-6003	Quartzite	70	67.81299	66.27107	460	2	Khynotayakha moraine	1.5233E+05	4.5700E+03	07KNSTD	23.94±0.72
09-6004	Quartzite	60	67.81285	66.27213	460	3	Khynotayakha moraine	1.6960E+05	5.0881E+03	07KNSTD	26.67±0.81
09-6005	Quartzite	55	67.81036	66.27656	438	4	Khynotayakha moraine	1.0977E+05	3.2931E+03	07KNSTD	17.60±0.53
09-6006	Quartzite	55	67.80989	66.27888	438	4	Khynotayakha moraine	1.6558E+05	4.9675E+03	07KNSTD	26.60±0.80
09-6007	Quartzite	50	67.80958	66.28013	436	3	Khynotayakha moraine	1.4960E+05	4.4879E+03	07KNSTD	24.07±0.73
09-6010	Quartzite	55	67.80500	66.34100	486	5	495 m hill	4.0574E+05	1.2172E+04	07KNSTD	62.80±1.91
09-6012	Quartzite	120	67.81738	66.33460	415	5	495 m hill	1.0654E+06	2.0242E+04	07KNSTD	182.06±3.63
07-7024	Quartz	170	67.80831	66.53364	140	5	Bol. Shchuchya valley	4.1276E+04	2.4821E+03	07KNSTD	8.87±0.54
07-7025	Quartzite	60	67.81100	66.54906	156	5	Bol. Shchuchya valley, gently undulating surface	2.6992E+05	6.2930E+03	07KNSTD	57.50±1.36
07-7026	Quartzite	45	67.80125	66.48694	177	5	Bol. Shchuchya valley, moraine	9.7548E+04	2.5570E+03	07KNSTD	20.15±0.53
07-5002	Quartzite	50	67.80275	66.43952	205	5	Mal. Shchuchya valley, moraine	2.9246E+05	6.8284E+03	07KNSTD	59.76±1.42
07-5004	Quartzite	50	67.79662	66.42968	210	5	Mal. Shchuchya valley, moraine	3.4432E+04	1.2662E+03	07KNSTD	6.92±0.25
07-5005	Quartzite	130	67.78205	66.28620	270	5	Mal. Shchuchya valley side	1.6815E+04	1.7310E+03	07KNSTD	3.12±0.32
07-5006	Quartzite	80	67.78207	66.28640	274	5	Mal. Shchuchya valley side	1.4119E+04	7.3458E+02	07KNSTD	2.62±0.14
09-7013	Gneiss	80	67.72601	66.96895	209	2	Gerdizshor valley, hill	1.8479E+05	4.6196E+03	07KNSTD	37.51±0.95
09-7014	Gneiss	60	67.73603	66.93859	226	2	Gerdizshor valley, moraine	1.5275E+05	3.9714E+03	07KNSTD	30.39±0.80
98-0034	Quartzite	130	68.126	65.73	580	3.5	Perekhvachennyi moraine	5.3255E+05	7.2695E+03	07KNSTD	29.4±0.9
98-0035	Quartzite	70	68.126	65.73	580	5	Perekhvachennyi moraine	1.6898E+05	5.2756E+03	07KNSTD	21.5±0.7

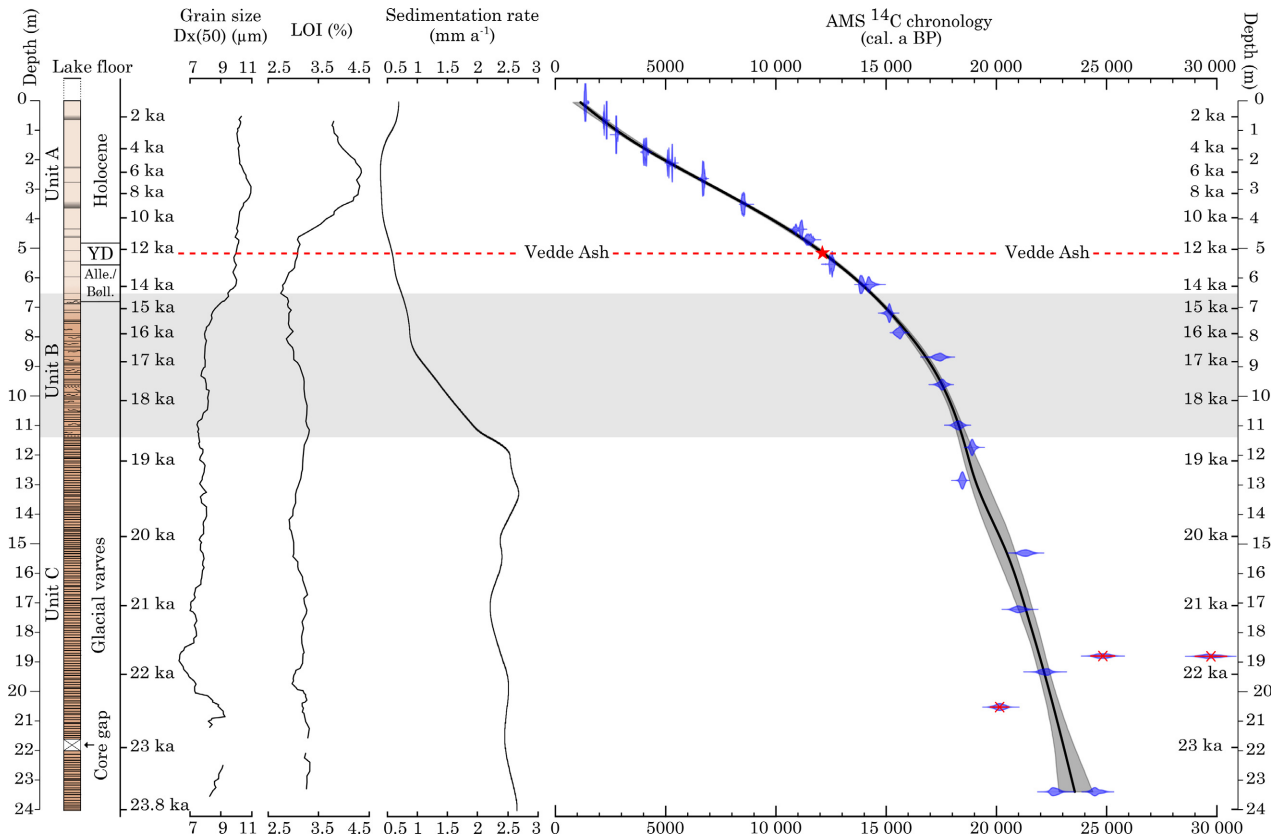

Fig. 8. Sediment stratigraphy and constructed age model of core 506-48. The calibrated radiocarbon dates that were obtained from this core are plotted with 95% confidence intervals. Only three radiocarbon ages, given in red, are more than 2 standard deviations outside the curve for the age model. Lithostratigraphical units (A–C), grain-size distribution, loss on ignition and calculated sedimentation rate are shown. The position of the Vedde Ash is marked with a red star and a dotted line. [Colour figure can be viewed at www.boreas.dk]

high lake level dates to 14–15 ka BP or perhaps even earlier.

Near the eastern boundary of the delta front on the north shore, there are some gravel terraces located only 2–3 m above the lake level (Fig. 10B). A clearing in one of the terraces showed slightly inclined layers of parallel laminated sand and gravel, which we interpreted as a beach deposit. Three OSL dates yielded 2.4±0.3, 3.2±0.4 and 3.8±0.4 ka (Table 2), indicating that the lake level was 2–3 m higher than today during the Late Holocene at around 2–4 ka ago.

Damming of the lake by a glacifluvial fan across the outlet

The outlet river presently runs across a bedrock sill at the southern end of the lake. However, as mentioned above the outlet river has apparently cut through a glacifluvial fan that earlier covered the entire threshold area, and it seems likely that this deposit once dammed the lake (Figs 3, 10A). The fan appears to have accumulated at the mouth of the tributary Sehrmalyakha Valley that leads up to the mountain valleys on the western side of Bol. Shchuchye. Several relict braided river channels that reached the southern end of the lake are found on the northern sector of the fan. We interpret the fan as a glacifluvial deposit that accumulated in front of a retreating ice tongue in the Sehrmalyakha Valley. The front of this glacier may have reached the bottom of the valley near the southern end of the lake. Some circular, water-filled, depressions on the lower part of the fan are considered to be kettleholes that formed when blocks of buried glacier ice melted. The braided palaeo-channels on the northern side of the mentioned fan flatten out towards a terrace 7–8 m above the present lake level, corresponding with the shoreline at this altitude. We therefore assume that the high lake level was caused by the fan that accumulated across the outlet and thereby dammed the lake. Samples from three boulders sitting in a former river channel near the highest point of the fan yielded ^{10}Be exposure ages of 14.5±0.7, 15.8±0.4 and 37.0±0.7 ka. We rely most on the youngest two dates as they gave roughly similar ages and suspect that the oldest date overestimates the real age of the depositional event, possibly inherited from an earlier period. Thus, we find it most likely that that the incision of the fan, and thereby also the lake lowering, started after 14–15 ka.

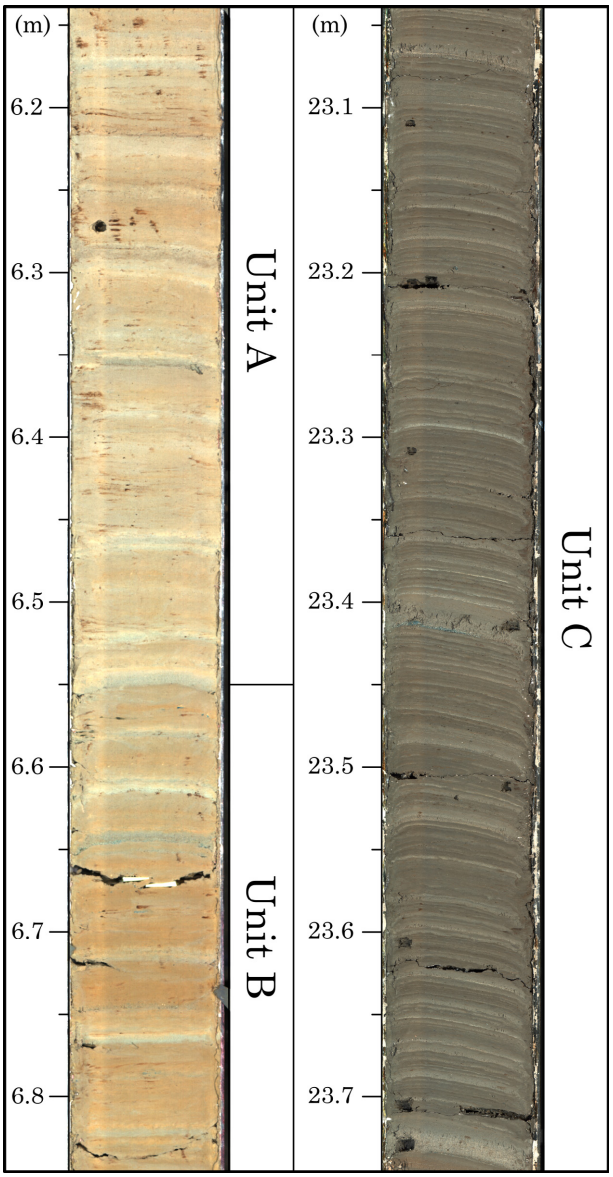

Fig. 9. Images of core 506-48 showing the strong lamination of unit C, interpreted as glacial varves, and a section of units A and B with a more diffuse lamination. [Colour figure can be viewed at www.boreas.dk]

Meltwater channels entering the southern end of the lake

Along the slopes of the mountains and within some of the valleys there are several fluvial channels and terraces that do not follow the natural drainage direction and which are interpreted to be the result of glacial meltwater erosion. Near the southern end of Bol. Shchuchye, several such channels extend northwards from the Sehrmalyakha Valley and across the watershed towards the lake. About 3 km northwest of the outlet, the largest of these channels (~1.5 km long) leads to the shore of Bol. Shchuchye (Figs 3, 10C). A little <200 m from the mouth of this channel it is incised 20–30 m into the otherwise flat bedrock plateau. Closer to the lake, the incision is split into two separate courses at different levels, showing that the upper one became dry first. In this highest, southernmost branch there is a 5-m-thick sequence of parallel bedded sand and gravel that dips slightly towards the lake (Fig. 10C); interpreted by us as glacifluvial sediments that accumulated in a meltwater river flowing towards the lake. The channel ends blindly at a 30-m-high cliff along the lake. As there is nothing to suggest that the lake level has been as much as 30 m higher than at present we assume the corresponding meltwater river flowed to the southeast along the margin of a former trunk glacier that filled the lake basin up to this level. Three OSL dates from this sediment sequence gave the ages 47±5, 60±6 and 124±11 ka. The ages are reversed in relation to their stratigraphical positions. A plausible explanation for these deviating dates may be that some quartz grains in the sample were not sufficiently bleached during transportation.

Alluvial fans along the present shore of the lake

Along the eastern shore of the lake, there are several prominent alluvial fans that have been deposited in front of ravines that are carved deeply into the steep bedrock valley sides (Figs 3, 4B). The seismic profiles suggest that these inclined deposits have been the source for many debrisflows in the lake (Haflidason *et al.* 2019a). The fan surfaces consist for the most part of coarse gravel and boulders. They are presently partly overgrown with vegetation, and especially in their upper reaches they are deeply incised by the streams that earlier formed them. We conclude that the fans are relict in the sense that they are no longer aggrading, but have undergone fluvial erosion for a rather long period of time. This is consistent with our interpretation that the lake level has been falling, but they probably also reflect a more plentiful supply of physically weathered material at an earlier date.

Source sediments in the main valley north of the lake

Bluffs and erosion scars along the Pyryantanë River Valley, the main valley draining into the lake from the north, demonstrate that the river has cut several metres into pre-existing alluvial gravel and sand deposits (Figs 3, 10D), perhaps partly as a response to a falling lake level. These large volumes of sand and gravel have contributed to progradation of the delta front in the northern end of the lake, whereas the fines have ended in deeper water.

In the northern part of the Pyryantanë Valley, near the watershed towards the Bol. Kara River on the western side of the Polar Urals, there is a sequence of terraces consisting of thick deposits of stratified sand and gravel that fills the valley floor in between bedrock outcrops (Figs 3, 10D). We interpret these deposits as outwash sediments that accumulated in front of one or several glaciers that terminated further upstream. Some circular

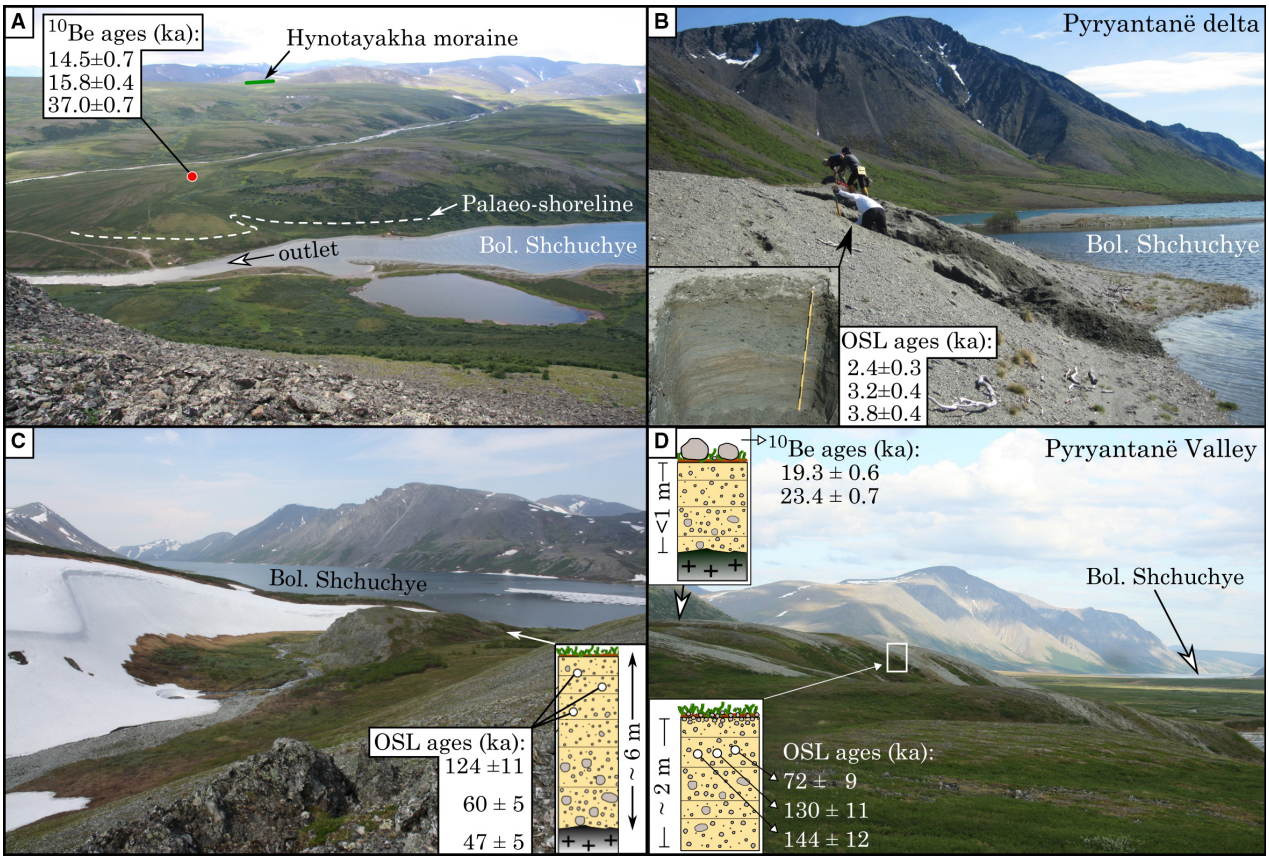

Fig. 10. A. Overview picture of the southern end of Bol. Shchuchye showing the outlet river and the glacifluvial fan at the mouth of Sehrmalyakha Valley. The fan has once dammed the lake. ^{10}Be dates (ka) from three exposed boulders sampled at the root point of the fan (red dot) are indicated. The position of the highest palaeo-shoreline (8 m above lake level) is marked with a dotted white line. The Hynotayakha moraine, from which five ^{10}Be dates were obtained, is marked with a green line at the watershed between the Sehrmalyakha and Hynotayakha river valleys (Fig. 13). B. Exposed beach sediments in a terrace that was investigated in the northern end of the lake. Three OSL ages (ka) obtained from this section are shown. C. Meltwater channel at the southwestern end of the lake. The channel contains a 5-m-thick sequence of stratified sand and gravel that was interpreted as a meltwater deposit. Three OSL dates (ka) that were obtained from this sequence of sand and gravel are shown. D. Overview picture of the Pyryantanë Valley seen towards the south from a terrace close to the water divide that leads over to the Bol. Kara Valley on the western side of the mountain range. Three OSL dates (ka) obtained from exposed sand and gravel near the top of the terrace are shown. Two ^{10}Be ages (ka) obtained from the surface of a corresponding terrace 600 m further to the north are also shown. [Colour figure can be viewed at www.boreas.dk]

depressions that occur on the valley floor are interpreted as kettleholes. Rivers have subsequently cut more than 20 m into the deposits and transported the sediments towards the lake. At least in one area, the terrace is strewn with rounded boulders and pebbles that must have been transported by running water. We obtained ^{10}Be ages of 23.4±0.7 and 19.3±0.6 ka from two rounded boulders that were collected from a place where a near horizontal bedrock platform is covered with a thin (0.5–1 m) layer of a coarse gravel (Fig. 10D). About 600 m south of this locality, and at a slightly lower level, there is a much thicker sequence of stratified sand and gravel above bedrock, interpreted as a glacifluvial outwash deposit. At this site, three OSL samples were obtained from the same stratigraphical level in a small clearing about 1 m below the surface (Fig. 10D). The dates yielded ages of 72±9, 130±11 and 144±12 ka. Considering that this most likely is a meltwater deposit it seems a likely possibility that some of the quartz grains were insufficiently bleached during transport and we therefore place most confidence in the youngest of the three ages. We suspect that the OSL-dated sand accumulated long before the ^{10}Be-dated boulders mentioned above. The latter dates suggest that the last time a meltwater river flowed down the valley at this high terrace level occurred during the LGM at around 23–19 ka or thereabouts, which implies that the fluvial incision started after this.

About 4 km further south in the Pyryantanë Valley, there is a large alluvial fan in front of the tributary Sangarehitosyo Valley (Fig. 3). Here, the Sangarehitosyo River has eroded a deep channel into the fan which most likely is a glacifluvial deposit. Near the upper root point of the fan, there is a narrow gravel terrace about 270 m a.s.l., which extends along the steep south-facing valley side. We assume this terrace corresponds to the

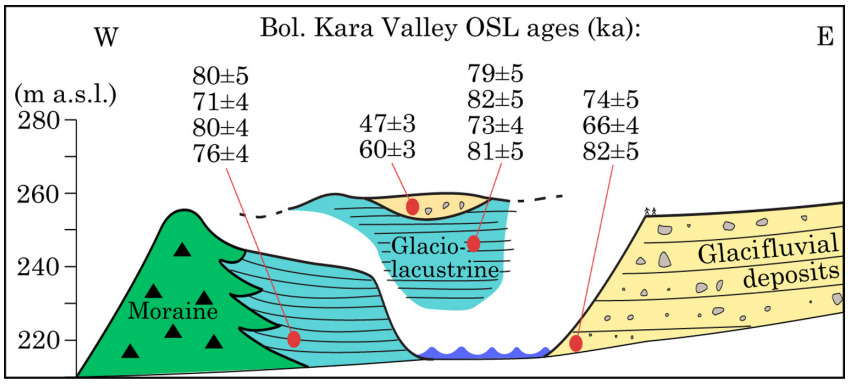

Fig. 11. Simplified geological profile with OSL ages (ka) across a moraine ridge in the Bol. Kara River Valley (see Fig. 2 for location). Upstream of the moraine (green) are laminated glaciolacustrine sediments (blue). The sediments in the terrace on the right side of the figure consist of coarse glacifluvial gravel with more fine-grained sand in the lower part from where three OSL dates were obtained. Two OSL dates were taken from a sequence of alluvial sediments above the glaciolacustrine formation in a nearby section. [Colour figure can be viewed at www.boreas.dk]

maximum expansion of the glacifluvial fan when the river in the main valley was level with the northern Pyryantanë Valley terraces mentioned above. Two water-transported boulders from the surface of the terrace gave ^{10}Be-dated ages of 18.9±0.5 and 11.3±0.3 ka. The oldest age fits well with the ^{10}Be age from the terrace further to the north in Pyryantanë Valley and it seems likely that the boulders were deposited by meltwater streams from glaciers that have occupied the mountain valleys further upstream.

Glaciolacustrine sediments in the Bol. Kara Valley west of the watershed

The Bol. Kara Valley starts at the watershed of the Pyryantanë River and descends westwards to the flat lowland along the flank of the mountain chain (Figs 2, 11). In the middle part of the valley, there is a prominent, 3-km-long and 20–30 m high, horseshoe-shaped moraine that clearly was deposited by an ice tongue flowing eastwards, i.e. upvalley. It is correlated with the Halmer Moraine on the lowland to the west and is assumed to have been deposited by the last shelf-centred ice sheet that reached the Polar Urals from the Kara Sea region (Fig. 1; Astakhov *et al.* 1999; Astakhov 2018).

On the eastern distal side of the moraine, a thick sequence of flat-lying laminated clay, silt and sand is exposed in river bluffs (Fig. 11). The laminated sediments must have accumulated in a lake that was dammed by an east-flowing ice tongue that blocked the westbound drainage. Just north of the moraine ridge (the right-hand section in Fig. 11) is a prominent river terrace developed in a thick sequence of coarse-grained glacifluvial gravel. The gravel, which presumably was deposited by meltwater streams flowing down the valley towards the lowland, covers more fine-grained sand and silt that appear near the base of the terrace escarpment. The interpretation of this lower unit is uncertain, but we tend to believe that it corresponds with the glaciolacustrine sediments that are exposed further to the west. We have conducted a series of eight OSL age estimates from sand layers within the laminated glaciolacustrine strata, all of them giving ages in the range 73–80 ka. Three samples that were taken from sand layers underneath the more coarse-grained glacifluvial gravel gave almost similar ages in the range 66–82 ka. Another two dates were obtained from younger fluvial sand and gravel that occur on top of the laminated lacustrine strata in a close-by section. These two dates were slightly younger at 60 and 47 ka, respectively (middle section, Fig. 11), and these ages are believed to post-date the last glaciation. This series of OSL ages indicates that the last ice-dammed lake that filled the inner part of the Kara Valley existed during MIS 4 and that this area has remained ice free since.

Moraines at the watershed SW of Bol. Shchuchye

On the floor of the east–west orientated main valley that crosses the watershed between Europe and Asia southwest of Bol. Shchuchye (Figs 2, 13) there is a 200–300 m long, 20–30 m wide and 3–8 m high moraine ridge that is parallel to the valley. In the southern end, it turns northwards across the valley, suggesting deposition from a glacier flowing out from the east-facing mountain side by the watershed. Three ^{10}Be ages of 13.2±0.4, 13.6±0.4 and 31.9±0.6 ka were obtained from boulders resting on top of the moraine. Two glacially transported boulders on the proximal side of the ridge gave divergent ages of 21.8±0.8 and 5.0±0.4 ka. The younger of the two clearly gives too young an age of the deglaciation. We also dated a boulder resting directly on bedrock on an isolated hill rising 100 m up from the valley bottom. It seems likely, although not proven, that this hill lay outside the glacier that deposited the above-mentioned moraine ridge. This boulder gave a much older age of 61.6±1.2 ka, suggesting that the hill has remained ice free since the beginning of MIS 3.

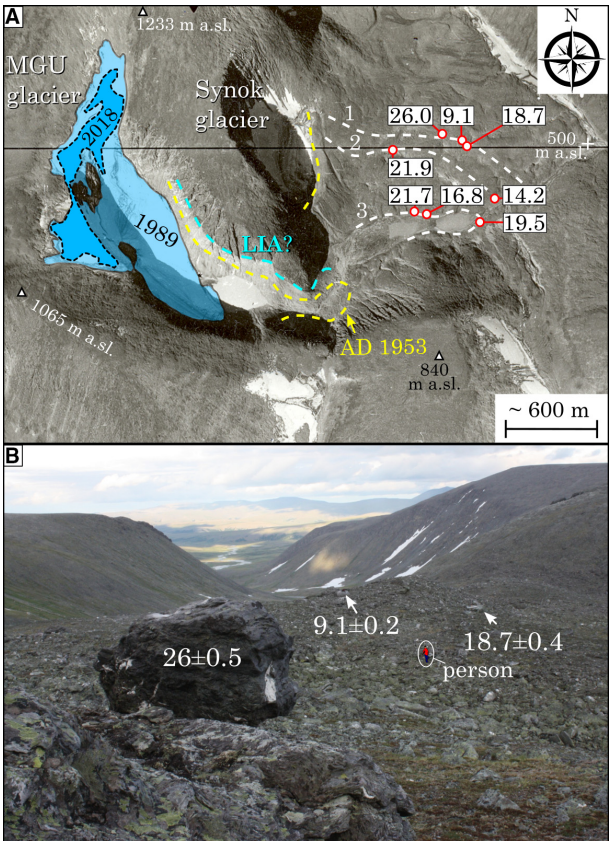

Fig. 12. A. Air photograph showing the present MGU glacier and the adjacent area. The extent of the glacier in 1953 (yellow) and older moraines (white dotted lines) that could be recognized in the forefield of the glacier are marked. Eight TCN ^{10}Be ages (ka) that were taken from boulders resting on three consecutive moraines (labelled 1–3) outside the 1953 ice-front position are shown. Also marked is the glacier extent in the years 1989 (when the air photograph was taken) and in 2018. The marked trimline just outside the 1953 margin is inferred to stem from a slightly earlier period, perhaps outlining the Little Ice Age glacier maximum. B. Photograph of moraine ridge in the forefield of the MGU glacier seen toward the east, away from the present glacier. Three ^{10}Be dates (ka) obtained from boulders from the outermost moraine (labelled 1 in (A)) are indicated. For scale, notice the person (in red) just inside the outermost moraine. [Colour figure can be viewed at www.boreas.dk]

Moraine ridges in the forefield of Moscow University Glacier (MGU) west of Mal. Shchuchye

Moscow University Glacier (MGU) is a tiny cirque glacier that in recent years has almost disappeared due to ongoing climate warming (Solomina *et al.* 2010). It is located at the heart of the narrow Gletcherny Valley about 5 km to the west of the lake Mal. Shchuchye (Figs 2, 12, 13). As late as AD 1953 this glacier stretched 2 km from its inner edge to the front. Just above the 1953 glacier margin, there is a very clear trimline from when the glacier was somewhat bigger. Considering that the mountain side up to the trimline is not overgrown with vegetation and lichens, we assume the withdrawal from this position did not happen long before 1953, most likely in the same century and in any case not before the end of the Little Ice Age.

In the forefield of the MGU glacier and a small adjacent cirque that is now ice free, there is a sequence of at least three consecutive moraine ridges that are located a short distance outside the maximum 20th century glacier extent (Fig. 12). All three ridges consist for the most part of clast-supported angular boulders and cobbles that only in places have a more fine-grained matrix (Færseth 2011). The outermost ridge, located about 1 km outside the ice-front position in 1953, is 20–30 m wide and 5–10 m high and forms an arc across the valley at altitudes from 740 m to 560 m a.s.l. About 50–100 m inside the crest of this outer moraine and parallel with it there is another, slightly smaller ice-pushed ridge. A few hundred metres further into the valley there is a third moraine ridge that bends around a small pond on the valley bottom. This one is 3–5 m high on the proximal side, but only 1–2 m on the distal side. The former ice tongue that deposited the inner ridge was much narrower than those that correspond with the two outer moraines and at this time it was no longer confluent with the smaller Synok cirque glacier that exists right next to the MGU glacier (Figs 12, 13).

In all, eight ^{10}Be dates were obtained from the above-mentioned moraine ridges. All of them were taken from the top surfaces of glacially transported boulders resting on other boulders below. There are three dates available from the outer moraine, two from the middle and three from the inner moraine (Figs 12, 13). The ages from the outermost of the three moraines were 26.0±0.5, 18.8±0.4 and 9.1±0.2 ka, while the two from the parallel ridge just inside were 14.2±0.3 and 21.9±0.4 ka. Those from the inner ridge were 21.7±0.4, 19.5±0.4 and 16.8±0.3 ka. In the field, we noted that the boulder that gave the youngest age (9.1±0.2 ka) from the outer ridge was less weathered than the others and this may suggest that it has moved since the moraine was formed. Despite the fact that there is some spread of ^{10}Be ages that we cannot fully explain, the data set demonstrates that all three ridges should be considered as retreat moraines that were deposited during the LGM (19–22 ka) or shortly afterwards.

Moraine ridge in the Hynotayakha Valley SW of Bol. Shchuchye

On a hillside midway between the southern ends of the two lakes Bol. Shchuchye and Mal. Shchuchye there is an 800–1000 m long ridge covered with boulders, cobbles and gravel at the surface (Figs 2, 13). The ridge, informally termed Hynotayakha moraine by us, is only some 2–3 m high and 50 m wide. It is located on a till surface at an elevation of 430–440 m a.s.l., close to the water divide between the Sehrmalyakha and Hynotayakha valleys. The shape, location and sediment composition suggest that this is a moraine. The ridge is cut through by a narrow gorge that must have been formed by meltwater running westward across a low pass between the two valleys. The

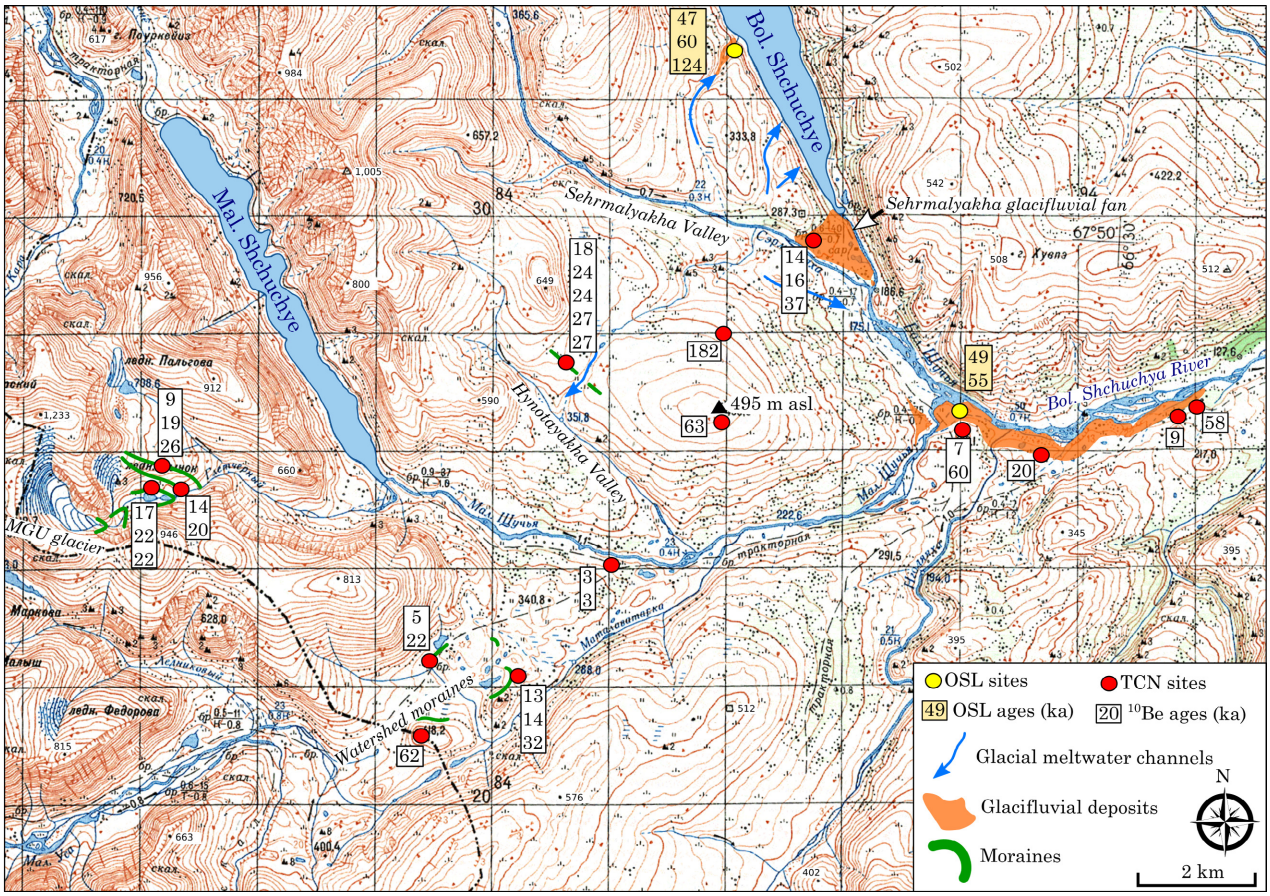

Fig. 13. Map of the area between Mal. Shchuchye and the southern end of Bol. Shchuchye. Moraine ridges (green streaks) and glacifluvial deposits (orange) are drawn on the map and all OSL (yellow dots) and ^{10}Be (red dots) ages (ka) that were obtained within this area are marked. Meltwater channels that lead into Bol. Shchuchye are shown with blue arrows. [Colour figure can be viewed at www.boreas.dk]

configuration of the glacier that formed the moraine is not clear, but we assume that it flowed down the Sehrmalyakha Valley and may have reached the southern end of Lake Bol. Shchuchye. ^{10}Be-dating of boulders resting on top of this moraine yielded four almost consistent ages of 26.7±0.7, 26.6±0.8, 24.1±0.7 and 24.0±0.7 ka whereas one was slightly younger at 17.6±0.5 ka (Fig. 14). The mean value of all five dates is 23.8±3.7 ka, or 25.3 ka if the young outlier (17.6±0.5 ka) is omitted. Two additional dates were obtained from a rounded mountain top just east of the moraine and topographically well above this ridge (Fig. 13); one erratic from the very summit (495 m a.s.l.) gave an age of 62.8±1.9 ka whereas a large boulder 50 m lower on the northern slope gave a much older age of 182±3.6 ka. Based on our knowledge of the glacial history, we believe the latter date gives too great an age for the last deglaciation, and we therefore suspect that this boulder has a legacy age from earlier ice-free periods. We consider that the former gives a more reasonable age for the deglaciation. Although there is uncertainty about this interpretation, the data set indicates that this summit was outside the reach of the glacier that deposited the Hynotayakha moraine.

Erratics and deltaic sediments along the Bol. Shchuchya River

We obtained five ^{10}Be dates from the river valley of Bol. Shchuchya 4–9 km downstream of the lake; all were taken from boulders protruding from some low mounds interpreted as remnants of moraines (Fig. 16). Two ages were nearly identical at 59.8±1.4 and 57.5±1.4 ka whereas the other three were much younger: 20.2±0.5, 6.9±0.3 and 8.9 ± 0.5 ka. The three latter dates are unrealistically young ages for the deglaciation and our interpretation is that the boulders became exposed long after this area became ice free, either by frost processes or running water (Heyman *et al.* 2011).

In a section along the outer bend of the river where it swings sharply to the east one can see steeply northwards-dipping foresets, covered by a metre-thick sequence of horizontally stratified gravel (Fig. 15). We interpret this sediment succession as a former deltaic deposit that accumulated in a shallow lake. This implies that the drainage towards the east must have been blocked, either by sediments or a glacier. Two OSL dates, one from the foresets and one from the overlying top-sets, were nearly identical at 55±4 and 49±4 ka, respectively. There were

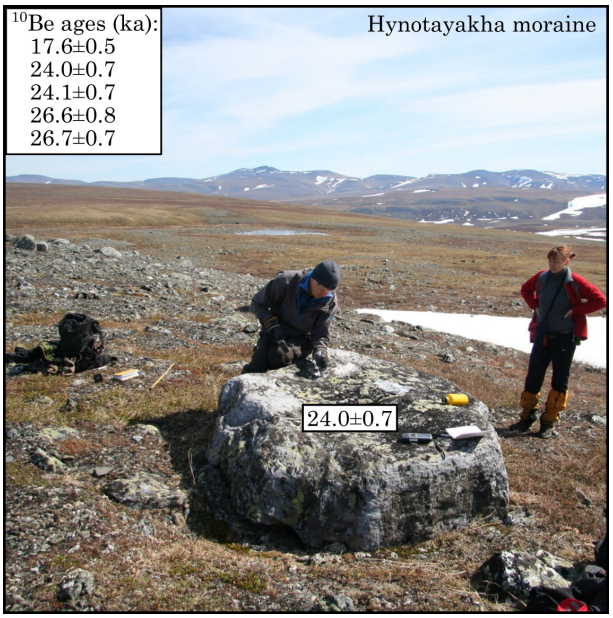

Fig. 14. Sampling for ^{10}Be dating (ka) along the Hynotayakha moraine ridge near the water divide between the Sehrmalyakha Valley and Hynotayakha Valley. The picture is taken towards the east. The ^{10}Be age (ka) that was obtained from this erratic is shown in the centre of the image and the whole series of dates from this moraine are shown in the frame at the top left. [Colour figure can be viewed at www.boreas.dk]

no tills or other proxies to suggest that the dated sediments had later on been overridden by glacier ice. Accordingly, these two OSL ages in combination with the two oldest ^{10}Be ages mentioned above suggest that the main valley became permanently ice free during an early stage of MIS 3, an assumption consistent with the age of deglaciation of the main valley slightly to the south (Mangerud *et al.* 2008a).

Erratics along the Gerdizshor River on the eastern side of the mountain range

Samples for ^{10}Be dating were collected from two glacially transported erratics from the Gerdizshor River Valley on the eastern foothills of the Polar Urals, about 27 km ESE of Bol. Shchuchye (Figs 2). One of the samples was collected from the top surface of a light grey erratic boulder of gneiss that rests directly on a bedrock outcrop at an elevation of 220 m a.s.l. (Fig. 16A). The sample gave an age of 37.5±0.9 ka. The other sample was also collected from a gneiss boulder, but this one was embedded in a lateral moraine located 1.7 km further to the NW and at an elevation of 223 m a.s.l. (Fig. 16B). The moraine ridge is 5–15 m high and stretches about 1 km from the NE to the SW. The sample from the boulder resting on this ridge yielded a slightly younger age of 30.4±0.8 ka. We cannot explain the age difference, but both of them suggest that a rather large glacier occupied the Gerdizshor Valley during a late stage of MIS 3.

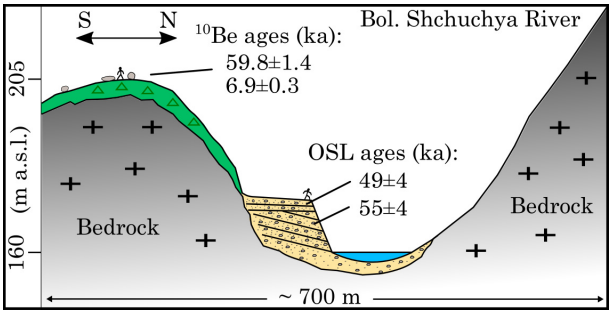

Fig. 15. Schematic geological profile across the Bol. Shchuchya River valley to the southeast of Bol. Shchuchye. The sketch shows deltaic sediments that are incised into a till surface. The ^{10}Be dates (ka) that were obtained from the till surface and OSL dates (ka) from an adjacent glacifluvial delta are shown. [Colour figure can be viewed at www.boreas.dk]

Enigmatic moraine ridge on the northern tip of the Polar Urals

At the northern tip of the Polar Urals, there is a distinct crescentic moraine ridge located at the mouth of a small valley in the 800–1000 m high Ochenyrd Mountains (Figs 2, 17). The moraine, which is about 1 km long and 20–30 m high, gently slopes from 585 m a.s.l. at the western side of the valley to 560 m a.s.l. near the eastern valley side. The ridge has an asymmetrical cross-profile

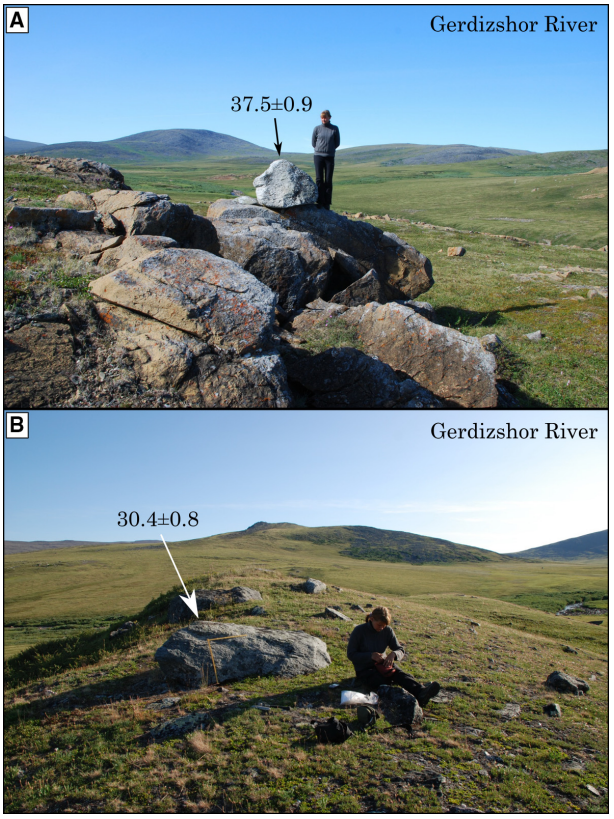

Fig. 16. Photographs of two ^{10}Be-dated boulders (ka) in the Gerdizshor River Valley on the eastern flank of the mountain chain. A. Erratic boulder resting on bedrock. B. Erratic boulder embedded in a moraine ridge. [Colour figure can be viewed at www.boreas.dk]

with the steepest slope facing north. Along the apex of the moraine lies a series of boulders of different sizes, many of them consisting of quartzite. The fact that the moraine ridge is slightly convex into the valley has previously been used to conclude that it was formed by an ice sheet flowing southwards from the continental shelf in the Barents and Kara Seas during an early stage of the last Ice Age (Astakhov *et al.* 1999; Astakhov 2014, 2018). ^{10}Be-dating of two large erratic boulders of quartzite embedded in the ridge yielded the ages 29.4±0.9 and 21.5±0.7 ka, which is inconsistent with the prevailing view that the northern tip of the Polar Urals and adjacent lowland has remained ice free since more than 50 ka ago (Svendsen *et al.* 2004; Astakhov 2014). We find it hard to reject these dates as they were conducted on large boulders considered to be well suited for exposure dating. However, we also find it very unlikely that the Barents-Kara Ice Sheet reached the Ural Mountains as late as during MIS 2 (Svendsen *et al.* 2004; Astakhov 2018). We therefore consider that these erratics, and probably the entire moraine, were deposited by a local glacier that during the peak of the MIS 2 glaciation lay in the valley upstream of the ridge. The fact that this moraine cannot be traced either further to the east or west along the mountain sides at this altitude (600–550 m a.s.l.) supports this interpretation.

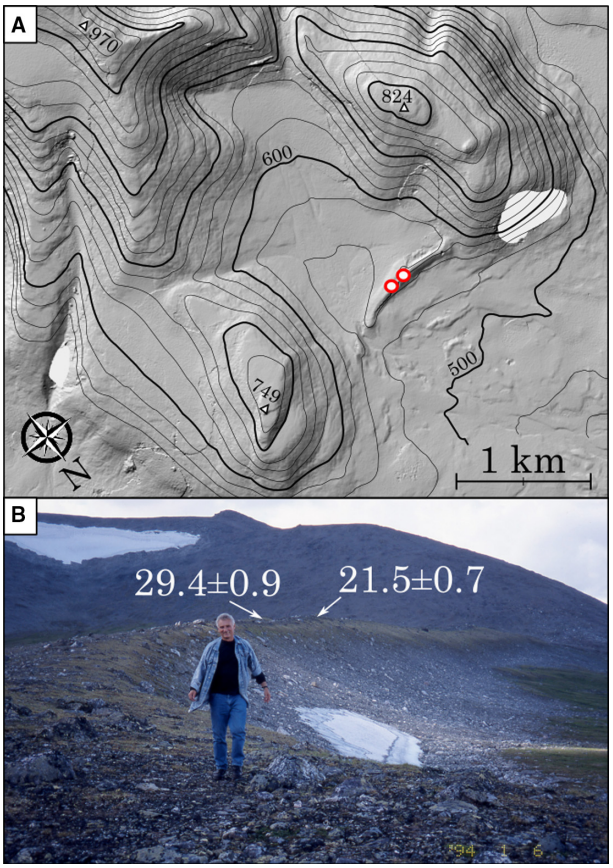

Fig. 17. A. Map of a cirque with a moraine ridge in the Ochenyrd Mountains at northern tip of the Polar Urals (for location see Fig. 2). B. Photograph of the moraine ridge (with Valery Astakhov) seen towards the west. Two ^{10}Be ages (ka) that were obtained from two erratic boulders resting on the moraine are marked. [Colour figure can be viewed at www.boreas.dk]

Discussion

Reliability of the dating results

In spite of a low content of organic matter, especially in the pre-Holocene part of the sequence, we consider that most of the radiocarbon dates provide reliable ages and that the age model for cores 506-48/50 provides a well-founded and precise chronological framework (Fig. 8). The Vedde Ash, identified at a sediment depth of 5.11–5.12 m in core 48 (Haflidason *et al.* 2019b), underpins the validity of the age model in this part of the core. According to our age model this level has an age of 12 122±160 cal. a BP, identical to the concluded age (12 121±57 cal. a BP) of this ash horizon in the Greenland ice-core stratigraphy (Andersen *et al.* 2006). It is also in agreement with the age (12 064±48 cal. a BP) of the Vedde Ash determined in the well-dated lake record from the site Kråkenes in western Norway (Lohne *et al.* 2013, 2014). The fact that there is a good match between the numbers of assumed annual layers and the radiocarbon ages from near the base of core 48 gives independent support for the validity of our age model (Regnéll *et al.* 2019).

Compared with the radiocarbon dates there is much greater uncertainty attached to the OSL and TCN exposure dates. Perhaps the biggest problem with the OSL dates is whether the quartz grains have been adequately exposed to sunlight (bleached) during transportation and deposition. If this is not the case the OSL dates overestimate the real ages. We suspect that incomplete bleaching explains some of the age range in our data set and as a general rule we attach most confidence to the youngest dates when there are deviating ages from the same stratigraphical context. However, experience suggests that OSL dating applied to glacifluvial and glaciolacustrine sediments in northern Russia in general gives reasonable ages (Thomas *et al.* 2006) and we think this is also the case here. However, the uncertainties are much larger than the error margins calculated from the laboratory measurements. Another potential source of error may be related to the water content in the sediments. The average water content measured in the sample from the glaciolacustrine sediments in the Bol. Kara Valley is 31%, which is 10% higher than the average of values measured for the remaining samples from the other sites. This difference may be real, but we note that a 1% decrease in average water/ice content leads to a ~1% decrease in age (Mangerud *et al.* 2001). Thus, if the average water content during the burial time has been 25%, the calculated ages would be 3–4000 years lower than reported here. In that case the OSL ages in this area would be more in accordance with our assumption that the glaciolacustrine sediments were deposited during MIS 4 and not during a previous period.

The TCN exposure dates, that in this study concern samples taken from boulders that were transported either by glacier ice or meltwater streams, also provide some large age distributions. For example, several of the dates are much younger than what is probable in the light of the current knowledge of the glacial chronology. We believe many of the abnormally young ages can be explained by freezing up of boulders long after the area became ice free and/or that they have been exposed as a result of fluvial erosion (Heyman *et al.* 2011; Alexanderson *et al.* 2014). Another potential source of error is that some of the boulders may have been recycled and may therefore have some inheritance from earlier exposure. This is especially relevant for areas with little bedrock erosion and long ice-free periods between the glaciations (Briner *et al.* 2016). We do not place much emphasis on individual ages when considering the chronologies, but look at the data set as a whole, and in particular we take into account localities where we have reasonably consistent series of ages, such as those obtained in the forefront of the MGU glacier and from the moraine ridge in the Hynotayakha Valley.

Sedimentation rates in the lake

The cored sediments consist almost exclusively of silt and clay deposited from suspension. Most of the sand and gravel was left in the fans along the lake and in the delta in the northern end; apparently most of the sediments were fed to the lake from the north. There are quite a few turbidite layers, especially in the Holocene sequence. However, in the southern end of the basin most turbidites are thin and fine-grained, although the lower parts contain coarser silt and also some sand. There is no evidence of disturbance or erosion underneath these layers in core 48/50. The seismic profiles show that fine-grained sediment units become thicker in the central part of the basin, as is common in most lakes (Fig. 6).

The age model shows that the sedimentation rates remained high and stable (2.2–2.6 mm a^{-1}) during the time interval 23.8–18.7 cal. ka BP, after which it gradually decreased until 11.6 cal. ka BP (Fig. 8). Despite this marked decline a relatively high sedimentation rate of 0.4–0.6 mm a^{-1} was maintained throughout the Holocene, although this is only about one-fifth of the rate during the LGM. We consider the Holocene rate unusual high because in cold Arctic climates with short ice-free summers the sediment supplies tend to be small unless there are glaciers in the catchment (Svendsen & Mangerud 1996). The relatively high sedimentation rate is probably due to a combination of several factors and processes that have operated at different time scales; one is the steep valley sides along the lake. The well-developed tors, at places several metres high, show that the steep bedrock valley sides are easily weathered and that weathering products are transported down to the lake by mass movements and running water, as seen in fans along the shores. There are, as described above, erosional escarpments in sand and gravel deposits in the valleys, especially in the main valley (Pyryantanë) north of the lake. The terraces testify that significant amounts of sediments have been eroded from the valley floors and brought into the lake by rivers.

The fact that the sedimentation rate is five times higher in the lower part of the cored sequence than in the Holocene interval is interpreted to reflect the glaciation history. We postulate that the exceptionally high sediment flux prior to 18.7 cal. ka BP is due to abundant sediment supply from meltwater rivers draining glaciers within the catchment. Below we briefly outline the glaciation history as we interpret it from the available data from the lake and the surrounding mountains.

A complex of large glaciers filling the central mountain valleys during MIS 4

We conclude that the data presented in this study support the assumption that the last major valley glaciers melted away 50–60 ka ago (Svendsen *et al.* 2014). At least some of the main valleys, including those crossing the mountain range, appear to have been permanently ice free since then. With the exception of one single ^{10}Be sample, which gave an unrealistically high age of 182 ka, all samples gave significantly younger ages but with a considerable spread. Four ^{10}Be samples gave ages in the range 57–63 ka, which are in good agreement with previous ages from both ^{10}Be and OSL dates from the western side of the mountain range (Mangerud *et al.* 2008a; Svendsen *et al.* 2014). Several ^{10}Be samples gave Holocene ages that without doubt are much too young for the last deglaciation. As mentioned above, considering that this is a permafrost region there is a risk that boulders became exposed by frost action and/or that they have been turned around by thawing and freezing processes (Heyman *et al.* 2011; Alexanderson *et al.* 2014). This has probably occurred with several of the boulders we have sampled. However, we note that those that have been lying directly on bedrock or on top of other large boulders gave higher ages and are considered the most reliable for reconstructing the glacial history.

There are no observations suggesting that the Barents-Kara Ice Sheet overran the Polar Urals during MIS 4, and we consider that the last glacier that filled the lake basin of Bol. Shchuchye was centred within the mountain range, with an ice divide located close to the watershed leading to the Bol. Kara Valley on the western side of the mountain rage. The fact that erratic boulders were deposited on the 495-m-high mountain top to the south end of Bol. Shchuchye suggests that the ice was more than 800 m thick in the lake basin (Figs 13, 18). During the peak of this glaciation, there is no doubt that this glacier must have flowed down the Bol. Kara Valley towards the western lowland. However, the prominent horseshoe-shaped moraine in this valley (Figs 2, 11) was deposited by a glacier flowing in the opposite direction, i.e.

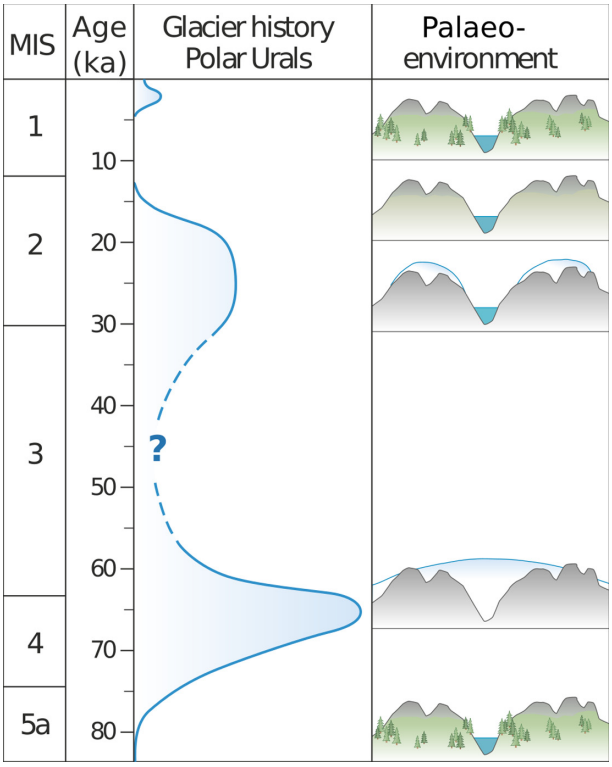

Fig. 18. Curve showing the growth and decay of glaciers in the Polar Urals since MIS 5a and a schematic reconstruction (cross-sections of the lake) for some selected time horizons. [Colour figure can be viewed at www.boreas.dk]

eastwards from the adjacent lowland. This was an ice tongue from the Barents-Kara Ice Sheet that streamed southwards along the western flank of the Polar Urals where it penetrated far into the Bol. Kara Valley. As a consequence, we conclude that the maximum extent of the last large mountain-centred glaciers pre-dates the maximum extent of the last ice-sheet advance from the Kara Sea shelf, although both are dated to MIS 4.

The up to 160-m-thick sediment sequence in Bol. Shchuchye has similar acoustic signatures all the way to the bottom, suggesting continuous sedimentation. We postulate that the last glacier that occupied the lake basin also removed older sediments that must have accumulated here during the foregoing ice-free period, i.e. that the existing lacustrine sediments started to accumulate as soon as the last glacier filling the basin melted away (Fig. 18). If we consider the sedimentation rates found in the lower half of the cores 48 and 50 and adjust for the downwards narrowing basin form, we find that the basal sediments have an age of about 50–60 ka (Haflidason *et al.* 2019a), consistent with other data suggesting that the last glaciation took place during MIS 4 or during an early stage of MIS 3.

A regrowth of the glaciers during MIS 3–2

We know little about the development of glaciers in the Polar Urals during the long period corresponding to MIS 3. The ^{10}Be ages of the two large boulders from the Gerdizshor River Valley, near the eastern foothills of the mountain range (Figs 2, 16), may suggest that there were quite large glaciers here in the period around 35–30 ka, i.e. well before the LGM. These two boulders, that evidently were transported and left on the ground by a former glacier, were designated by us to be amongst the best dating objects collected during the field campaign. The suspicion that relatively large mountain glaciers existed in a late phase of MIS 3 is in line with the fact that rivers draining the mountain range seem to have been large at this time, possibly due to an abundant supply of meltwater from glaciers (Mangerud *et al.* 1999; Svendsen & Pavlov 2003; Svendsen *et al.* 2014).

As is apparent from the dating results, there is good evidence to suggest that quite a few mountain glaciers existed during MIS 2 and some of them expanded well out of the shady cirques that host the recent glaciers (Figs 12, 13, 18). Perhaps the most convincing argument in favour of this hypothesis is the five consistent ^{10}Be dates from the Hynotayakha Moraine with a mean age of 23.8 ka (Fig. 14, Table 3). This age is considered a minimum age of the corresponding glacier. The location of this moraine suggests that the corresponding glacier must have been quite large and it seems a likely possibility that it reached the southern end of Lake Bol. Shchuchye (Fig. 13). By comparison, it appears that the MGU glacier in the Gletcherny Valley to the east of the lake basin of Mal. Shchuchye was only slightly larger during the LGM than in 1953. We have no good explanation as to why this glacier appears to have been much smaller than the glacier that deposited the Hynotayakha Moraine mentioned above. We cannot ignore the possibility that the Gletcherny Valley hosted a larger glacier just prior to the LGM, although we have not found geomorphological traces to suggest that the glacier then reached further down the valley.

Core 48 from the southern end of the lake stops just above a distinct reflector that marks the top of a seismic unit with a chaotic internal structure (Fig. 6) and, as mentioned above, scratches on the piston indicates that it contains a lot of coarse rock material. This unit could be the result of mass movements, but we find no source for a landslide in this particular area. We are therefore open to the possibility that the coarse-grained sediments originated from the same glacier that deposited the Hynotayakha Moraine, i.e. that the ice front during its maximum extent reached all the way to the southern end of the lake. In this regard we find it striking that the age of the basal lacustrine sediments in core 48 is almost identical to the ^{10}Be ages that were obtained from the Hynotayakha moraine reported above (Figs 13, 14). This again suggests that the glacier expansion culminated before 24 cal. ka BP, either during an early phase of MIS 2 or late stage of MIS 3.

The glacifluvial deposits to the north of the lake also suggest that there were glaciers in several of the higher

mountain valleys and cirques during the LGM or thereabouts. Furthermore, some of the ^{10}Be ages (13.3, 13.6, 21.8, 31.9 ka) that were obtained from the moraines at the water divide southwest of Bol. Shchuchye may suggest that small glaciers formed on the east-facing mountain slopes also in this area. Some 20 km further southwest the small Chernov Glacier expanded only about 1 km during the LGM (Mangerud *et al.* 2008a). The cored sequence reveals a persistent fast sedimentation rate (2.2–2.6 mm a^{-1}) during the period between 23.8 and 18.7 cal. ka BP, corresponding with the period of varve formation (Regnéll *et al.* 2019). We postulate that this reflects the presence of sizeable glaciers in the catchment providing sediment-loaded meltwater to the lake. This is supported by the ^{10}Be dates and we postulate that a large number of glaciers existed in the mountains during this period, but the main valleys appear to have been ice free (Fig. 18). The marked decrease in sedimentation rate that started 18–17 ka BP is probably due to the fact that the glaciers in the catchment then stared to melt back and were probably completely gone by 15–14 cal. ka BP. Throughout most of the Holocene, there were no glaciers in the Polar Urals and the recent small glaciers that exist in some shady cirques probably formed in response to the Late Holocene cooling.

Changes in lake level

Shorelines and terraces show that the water level in the lake has been up to 8 m higher than today (Fig. 10A), probably because it was dammed by a glacifluvial fan that expanded across the bedrock threshold in the southern end of the lake. Exposure ages of fluvially transported boulders at the root point of this fan suggest that the high lake level stand occurred at around 14–15 ka, but ^{10}Be dating of water-transported boulders on high-lying terraces in the valley to the north of the lake may suggest that it was high also during the LGM time. The lake level then dropped as the outlet river started to incise the damming fan. It is tempting to assume that this happened as soon as the sediment supply declined in response to the deglaciation. However, it should be noted that the timing of the lowering is not well constrained by dates. No matter how fast the downcutting has been, OSL dating of a low terrace in the northeastern corner of the lake reveals that the water level was 2–3 m higher than today some 2–3 ka ago.

Several of the seismic cross-profiles show some narrow underwater ledges along the slopes of the basin that can be perceived as former beach terraces (Haflidason *et al.* 2019a) and thus indicating a lower lake level. However, these features cannot be traced over long stretches and they appear at various depths through the basin, from 23 m and down to about 50 m below the present lake level. We are therefore reluctant to interpret these ledges as former beach levels. At any rate, if the lake level has been significantly lower than today it most likely happened during a dry period soon after the LGM (Siegert & Dowdeswell 2004; Heggen *et al.* 2012), but before the onset of the lateglacial interstadial of 14–15 cal. ka BP. There are also no indications that the lake level was low in the Holocene.

Conclusions

- Lake Bol. Shchuchye contains up to 160-m-thick lacustrine sediments that have accumulated since the last time the entire lake basin was covered by glacier ice.
- A series of 27 ^{14}C dates and a sequence of annual lamination in a 24-m-long sediment core retrieved from the southern part of the lake show that the cored sequence accumulated over the last 24 ka without any breaks or disturbances.
- Based on seismic correlation and extrapolation of the sedimentation rate it is inferred that the basin last was emptied of sediments by a former glacier just prior to 50–60 ka.
- Dating results from the surrounding areas indicate the main valleys in the Polar Urals were occupied by a complex of extended glaciers during MIS 4 (65–75 ka) that later melted back during an early stage of MIS 3 (Fig. 18).
- ^{10}Be dating of boulders resting on end moraines shows that there were a number of more restricted mountain glaciers during MIS 2 and probably also during a late stage of MIS 3.
- The high sedimentation rate (2.5 mm a^{-1}) of silt and clay in Bol. Shchuchye from 24 cal. ka BP until about 15–14 cal. ka BP reflects a significant contribution of mud from glacial meltwater from surrounding mountain glaciers that existed at this time.
- A pronounced decrease in the sedimentation that took place between 18–15 cal. ka BP is assumed to reflect a comprehensive deglaciation when most, if not all glaciers in the catchment area melted away.

Acknowledgements. – This work was financially supported by The Research Council of Norway and is a contribution to the projects 'Climate History along the Arctic Seaboard of Eurasia' (CHASE; NRC 255415) and 'Eurasian Ice Sheet and Climate Interaction' (EISCLIM; NCR 229788). The fieldwork and the coring of Lake Bol. Shchuchye were carried out in 2007 and 2009 during the former research project 'Ice Age Development and Human Settlement in Northern Eurasia' (ICEHUS) funded by the Research Council of Norway (NCR 167131 and NCR 176176048). The sediment analyses were performed at the National Infrastructure EARTHLAB (NRC 336171) at the University of Bergen. Eva Bjørseth at the Department of Earth Science, University of Bergen, prepared some of the illustrations. Ívar Örn Benediktsson and an anonymous reviewer provided useful comments and suggestions that helped to improve the quality of the manuscript. We offer our sincere thanks to all who have contributed to this study. This study is also a contribution to the Bjerknes Centre for Climate Research in Bergen. J. M. Schaefer acknowledges support by the Lamont Climate Centre. This is LDEO publication #8255.

References

Alexanderson, H., Backman, J., Cronin, T. M., Funder, S., Ingólfsson, Ó., Jakobsson, M., Landvik, J. Y., Löwemark, L., Mangerud, J., März, C., Möller, P., O'Regan, M. & Spielhagen, R. F. 2014: An Arctic perspective on dating Mid-Late Pleistocene environmental history. *Quaternary Science Reviews 92*, 9–31.

Andersen, K. K., Svensson, A., Johnsen, S. J., Rasmussen, S. O., Bigler, M., Röthlisberger, R., Ruth, U., Siggaard-Andersen, M.-L., Steffensen, J. P., Dahl-Jensen, D., Vinther, B. M. & Clausen, H. B. 2006: The Greenland Ice Core Chronology 2005, 15-42 ka. Part 1: constructing the time scale. *Quaternary Science Reviews 25*, 3246–3257.

Andreev, A. A., Tarasov, P. E., Ilyashuk, B. P., Ilyashuk, E. A., Cremer, H., Hermichen, W. D., Wischer, F. & Hubberten, H. W. 2005: Holocene environmental history recorded in Lake Lyadhej-To sediments, Polar Urals, Russia. *Palaeogeography, Palaeoclimatology, Palaeoecology 223*, 181–203.

Astakhov, V. I. 2013: Pleistocene glaciations of northern Russia – a modern view. *Boreas 42*, 1–24.

Astakhov, V. I. 2014: The postglacial Pleistocene of northern Russian mainland. *Quaternary Science Reviews 92*, 388–408.

Astakhov, V. I. 2016: Glaciomorphological map of the Russian Federation. *Quaternary International 420*, 4–14.

Astakhov, V. I. 2018: Late Quaternary glaciation of the northern Urals: a review and new observations. *Boreas 47*, 379–389.

Astakhov, V. I. & Nazarov, D. 2010: Correlation of Upper Pleistocene sediments in northern West Siberia. *Quaternary Science Reviews 29*, 3615–3629.

Astakhov, V. I. & Svendsen, J. I. 2002: Age of remnants of a Pleistocene glacier in the Bolshezemelskaya Tundra. *Doklady Earth Sciences 384*, 468–472.

Astakhov, V. I., Arslanov, Kh. A. & Nazarov, D. V. 2004: The age of mammoth fauna on the Lower Ob. *Doklady Earth Sciences 396*, 538–542.

Astakhov, V. I., Svendsen, J. I., Matiouchkov, A., Mangerud, J., Maslenikova, O. & Tveranger, J. 1999: Marginal formations of the last Kara and Barents ice sheets in northern European Russia. *Boreas 28*, 23–45.

Balco, G., Briner, J., Finkel, R. C., Raybum, J. A., Ridge, J. C. & Schaefer, J. M. 2009: Regional beryllium-10 production rate calibration for late-glacial northeastern North America. *Regional Geomorphology 4*, 93–107.

Balco, G., Stone, J. O., Lifton, N. A. & Dunnai, T. J. 2008: A complete and accessible means of calculating surface exposure ages or erosion rates from ^{10}Be and ^{26}Al measurements. *Quaternary Geochronology 3*, 174–195.

Blaauw, M. 2010: Methods and code for 'classical' age-modelling of radiocarbon sequences. *Quaternary Geochronology 5*, 512–518.

Briner, J. P., Goehring, B. M., Mangerud, J. & Svendsen, J. I. 2016: The deep accumulation of ^{10}Be at Utsira, southwestern Norway: implications for cosmogenic nuclide exposure dating in peripheral ice sheet landscapes. *Geophysical Research Letters 43*, 9121–9129.

Croudace, I. W., Rindby, A. & Rothwell, R. G. 2006: ITRAX: description and evaluation of a new multi-function X-ray core scanner. *Geological Society, London, Special Publications 267*, 51–63.

Dushin, V. A., Serdyukova, O. P., Malyugin, A. A., Nikulina, I. A., Kozmin, V. S., Burmako, P. L., Abaturova, I. V. & Kozmina, L. I. 2009: *State Geological Map of the Russian Federation 1:200 000. Polar Ural Series. Sheet Q-42-I, II (Laborovaya)*. VSEGEI, St. Petersburg (in Russian).

Færseth, L. M. 2011: *Glaciations in the Bolshaya and Malaya Shutchye area, the Polar Urals*. M.Sc. thesis, Norwegian University of Life Science, 65 pp.

Gosse, J. C. & Phillips, F. M. 2001: Terrestrial in situ cosmogenic nuclides: theory and application. *Quaternary Science Reviews 20*, 1475–1560.

Haflidason, H., Zweidorff, J. L., Baumer, M., Gyllencreutz, R., Svendsen, J. I., Gladysh, V. & Logvina, E. 2019a: The Last Glacial and Holocene seismostratigraphy and sediment distribution of the Lake Bolshoye Shchuchye, Polar Ural Mountains, Arctic Russia. *Boreas 48*, 452–469.

Haflidason, H., Regnéll, C., Pyne-O'Donnell, S. & Svendsen, J. I. 2019b: Extending the known distribution of the Vedde Ash into Siberia: occurrence in lake sediments from the Timan Ridge and the Ural Mountains, northern Russia. *Boreas 48*, 444–451.

Heggen, H. P., Svendsen, J. I., Mangerud, J. & Lohne, Ø. S. 2012: A new palaeoenvironmental model for the evolution of the Byzovaya Palaeolithic site, northern Russia. *Boreas 41*, 527–545.

Henriksen, M., Mangerud, J., Maslenikova, O., Matiouchkov, A. & Tveranger, J. 2001: Weichselian stratigraphy and glaciotectonic deformation along the lower Pechora River, Arctic Russia. *Global and Planetary Change 31*, 295–317.

Henriksen, M., Mangerud, J., Matiouchkov, A., Murray, A. S., Paus, A. & Svendsen, J. I. 2008: Intriguing climatic shifts in a 90 kyr old lake record from northern Russia. *Boreas 37*, 20–37.

Henriksen, M., Mangerud, J., Matiouchkov, A., Paus, A. & Svendsen, J. I. 2003: Lake stratigraphy implies an 80 000 yrs delayed melting of buried dead ice in northern Russia. *Journal of Quaternary Science 18*, 663–679.

Heyman, J., Stroeven, A. P., Harbor, J. M. & Caffee, M. W. 2011: Too young or too old: evaluating cosmogenic exposure dating based on an analysis of compiled boulder exposure ages. *Earth and Planetary Science Letters 302*, 71–80.

Hubberten, H. W., Andreev, A., Astakhov, V. I., Demidov, I., Dowdeswell, J. A., Henriksen, M., Hjort, C., Houmark-Nielsen, M., Jakobsson, M., Kuzmina, S., Larsen, E., Lunkka, J. P., Lysså, A., Mangerud, J., Möller, P., Saarnisto, M., Schirrmeister, L., Sher, A. V., Siegert, C., Siegert, M. J. & Svendsen, J. I. 2004: The periglacial climate and environment in northern Eurasia during the Last Glaciation. *Quaternary Science Reviews 23*, 1333–1357.

Hufthammer, A. K., Svendsen, J. I. & Pavlov, P. 2019: Animals and humans in the European Russian Arctic towards the end of the last Ice Age and during the mid-Holocene time. *Boreas 48*, 387–406.

Hughes, A. L., Gyllencreutz, R., Lohne, Ø. S., Mangerud, J. & Svendsen, J. I. 2016: The last Eurasian ice sheets – a chronological database and time-slice reconstruction, DATED-1. *Boreas 45*, 1–45.

Lammers, Y., Clark, C., Erséus, C., Brown, A., Edwards, M. E., Gielly, L., Haflidason, H., Mangerud, J., Svendsen, J. I. & Alsos, I. G. 2019: Clitellate worms (Annelida) in lateglacial and Holocene sedimentary DNA records from the Polar Urals and northern Norway. *Boreas 48*, 317–329.

Larsen, E., Kjær, K. H., Demidov, I. N., Funder, S., Grøsfjeld, K., Houmark-Nielsen, M., Jensen, M., Linge, H. & Lysså, A. 2006: Late Pleistocene glacial and lake history of north-western Russia. *Boreas 35*, 394–424.

Lohne, Ø. S., Mangerud, J. & Birks, H. H. 2013: Precise ^{14}C ages of the Vedde and Saksunarvatn ashes and the Younger Dryas boundaries from western Norway and their comparison with the Greenland Ice Core (GICC05) chronology. *Journal of Quaternary Science 28*, 490–500.

Lohne, Ø. S., Mangerud, J. & Birks, H. H. 2014: IntCal13 calibrated ages of the Vedde and Saksunarvatn ashes and the Younger Dryas boundaries from Kråkenes, western Norway. *Journal of Quaternary Science 29*, 506–507.

Mangerud, J., Astakhov, V. I., Murray, A. & Svendsen, J. I. 2001: The chronology of a large ice-dammed lake and the Barents-Kara Ice Sheet advances, Northern Russia. *Global and Planetary Change 31*, 321–336.

Mangerud, J., Gosse, J., Matiouchkov, A. & Dolvik, T. 2008a: Glaciers in the Polar Urals, Russia, were not much larger during the Last Global Glacial Maximum than today. *Quaternary Science Reviews 27*, 1047–1057.

Mangerud, J., Jakobsson, M., Alexanderson, H., Astakhov, V., Clarke, G. K. C., Henriksen, M., Hjort, C., Krinner, G., Lunkka, J.-P., Möller, P., Murray, A., Nikolskaya, O., Saarnisto, M. & Svendsen, J. I. 2004: Ice-dammed lakes and rerouting of the drainage of northern Eurasia during the Last Glaciation. *Quaternary Science Reviews 23*, 1313–1332.

Mangerud, J., Kaufman, D., Hansen, J. & Svendsen, J. I. 2008b: Ice free conditions on Novaya Zemlya 35 000-30 000 cal. years B.P., as indicated by radiocarbon ages and amino acid racemization evidence from marine molluscs. *Polar Research 37*, 182–208.

Mangerud, J., Lie, S. E., Furnes, H., Kristiansen, I. L. & Lømo, L. 1984: A Younger Dryas ash bed in western Norway, and its possible correlation with tephra in cores from the Norwegian Sea and the North Atlantic. *Quaternary Research 21*, 83–104.

Mangerud, J., Svendsen, J. I. & Astakhov, V. I. 1999: Age and extent of the Barents and Kara ice sheets in Northern Russia. *Boreas 28*, 46–80.

Möller, P., Alexanderson, H., Funder, S. & Hjort, C. 2015: The Taimyr Peninsula and the Severnaya Zemlya archipelago, Arctic Russia: a synthesis of glacial history and palaeo-environmental change during the Last Glacial cycle (MIS 5e–2). *Quaternary Science Reviews 107*, 149–181.

Murray, A. S. & Wintle, A. G. 2000: Luminescence dating of quartz using an improved single-aliquot regenerative-dose protocol. *Radiation Measurements 32*, 57–73.

Paus, A., Svendsen, J. I. & Matiouchkov, A. 2003: Late Weichselian (Valdaian) and Holocene vegetation and environmental history of the northern Timan Ridge, European Arctic Russia. *Quaternary Science Reviews 22*, 2285–2302.

Pavlov, P. Y., Svendsen, J. I. & Indrelid, S. 2001: Human presence in the European Arctic nearly 40,000 years ago. *Nature 413*, 64–67.

Pitulko, V., Pavlova, E. & Nikolskiy, P. 2017: Revising the archaeological record of the Upper Pleistocene Arctic Siberia: human dispersal and adaptations in MIS 3 and 2. *Quaternary Science Reviews 165*, 127–148.

Regnéll, C., Haflidasson, H., Mangerud, J. & Svendsen, J. I. 2019: Glacial and climate history of the last 24 000 years in the Polar Ural Mountains, Arctic Russia, inferred from partly varved lake sediments. *Boreas 48*, 432–443.

Reimer, P. J., Bard, E., Bayliss, A., Beck, J. W., Blackwell, P. G., Bronk Ramsey, C., Buck, C. E., Cheng, H., Edwards, R. L., Friedrich, M., Grootes, P. M., Guilderson, T. P., Haflidason, H., Hajdas, I., Hatté, C., Heaton, T. J., Hoffmann, D. L., Hogg, A. G., Hughen, K. A., Kaiser, K. F., Kromer, B., Manning, S. W., Niu, M., Reimer, R. W., Richards, D. A., Scott, E. M., Southon, J. R., Staff, R. A., Turney, C. S. M. & van der Plicht, J. 2013: IntCal13 and Marine13 radiocarbon age calibration curves 0–50,000 years cal BP. *Radiocarbon 55*, 1869–1887.

Sand, G. O. 2011: *Lake sedimentation and climate development in Polar Ural Mountains.* M.Sc. thesis, University of Bergen, 64 pp.

Schaefer, J. M., Denton, G. H., Kaplan, M., Putnam, A., Finkel, R. C., Barrell, D. J. A., Andersen, B. G., Schwartz, R., Mackintosh, A., Chinn, T. & Schlüchter, C. 2009: High-frequency Holocene glacier fluctuations in New Zealand differ from northern signature. *Science 324*, 622–625.

Schirrmeister, L., Grosse, G., Wetterich, S., Overduin, P. P., Strauss, J., Schuur, E. A. G. & Hubberten, W.-H. 2011: Fossil organic matter characteristics in permafrost deposits of the northeastern Siberian Arctic. *Journal of Geophysical Research: Biogeosciences 116*, 3–25, https://doi.org/10.1029/2011 JG01647.

Sher, A. V., Kuzmina, S. A., Kuznetsova, T. V. & Sulerzhitsky, L. D. 2005: New insights into the Weichselian environment and climate of the East Siberian Arctic, derived from fossil insects, plants, and mammals. *Quaternary Science Reviews 24*, 533–569.

Siegert, M. J. & Dowdeswell, J. A. 2004: Numerical reconstructions of the Eurasian Ice Sheet and climate during the Late Weichselian. *Quaternary Science Reviews 23*, 1273–1283.

Slimak, L., Svendsen, J. I., Mangerud, J., Plisson, H., Heggen, H. P., Brugère, A. & Pavlov, P. Y. 2011: Late Mousterian Persistence near the Arctic Circle. *Science 332*, 841–845.

Solomina, O., Ivanov, M. & Bradwell, T. 2010: Lichenometric studies on moraines in the Polar Urals. *Geografiska Annaler 92A*, 81–99.

Stuiver, M., Reimer, P. & Reimer, R. 2017: *CALIB 7.1.* Available at: http://calib.org/calib/ (accessed 01.03.2017).

Svendsen, J. I. & Mangerud, J. 1996: Holocene glacial and climate variations on Spitsbergen, Svalbard. *The Holocene 7*, 745–757.

Svendsen, J. I. & Pavlov, P. 2003: Mamontovaya Kurya: an enigmatic, nearly 40 000 years old Paleolithic site in the Russian Arctic. *In* Zilhao, J. & d′Errico, F. (eds.): *The Chronology of the Aurignacian and of the Transtional Ttechnocomplexe*, 109–120. Proceedings XIV UISPP Congress, University of Liège, Liège, Belgium.

Svendsen, J. I., Alexanderson, H., Astakhov, V. I., Demidov, I., Dowdeswell, J. A., Funder, S., Gataullin, V., Henriksen, M., Hjort, C., Houmark-Nielsen, M., Hubberten, H. W., Ingólfson, O., Jakobsson, M., Kjær, K. H., Larsen, E., Lokrantz, H., Lunkka, J. P., Lysså, A., Mangerud, J., Matiouchkov, A., Murray, A., Möller, P., Niessen, F., Nikolskaya, O., Polyak, L., Saarnisto, M., Siegert, C., Siegert, M. J., Spielhagen, R. F. & Stein, R. 2004: Late Quaternary ice sheet history of Northern Eurasia. *Quaternary Science Reviews 23*, 1229–1271.

Svendsen, J. I., Heggen, H. P., Hufthammer, A. K., Mangerud, J., Pavlov, P. & Roebroeks, W. 2010: Geo-archaeological investigations of Palaeolithic sites along the Ural Mountains - On the northern presence of humans during the last Ice Age. *Quaternary Science Reviews 29*, 3138–3156.

Svendsen, J. I., Krüger, L. C., Mangerud, J., Astakhov, V. I., Paus, A., Nazarov, D. & Murray, A. 2014: Glacial and vegetation history of the Polar Ural Mountains in northern Russia during the Last Ice Age, Marine Isotope Stages 5-2. *Quaternary Science Reviews 92*, 409–428.

Thomas, P.J., Murray, A.S., Kjær, K.H., Funder, S. & Larsen, E. 2006: Optically Stimulated Luminescence (OSL) dating of glacial sediments from Arctic Russia. *Boreas 35*, 587–599.

Troitsky, S. L., Hodakov, V., Mihalev, V., Guskov, A., Lebedeva, I., Adamenko, V. & Jivkovitch, I. 1966: *Glaciation of the Urals. Glaciology.* 308 pp. IV Section of the IGY program, vol. 16. NAUKA Akademia, Moscow (in Russian).

Väliranta, M., Kultti, S. & Seppä, H. 2006: Vegetation dynamics during the Younger Dryas-Holocene transition in the extreme northern taiga zone, northeastern European Russia. *Boreas 35*, 202–212.

Vasil'chuk, Y. K., van der Plicht, J., Jungner, H. & Vasil'chuk, A. C. 2000: AMS-dating of Late Pleistocene and Holocene syngenetic ice-wedges. *Nuclear Instruments and Methods in Physics Research B 172*, 637–641.

Young, N. E., Schaefer, J. M., Briner, J. P. & Goehring, B. M. 2013: A ^{10}Be production rate calibration for the Arctic. *Journal of Quaternary Science 28*, 515–526.